© 2016. Published by The Company of Biologists Ltd | Development (2016) 143, 787-798 doi:10.1242/dev.128553

RESEARCH ARTICLE

Tpbpa-Cre-mediated deletion of TFAP2C leads to deregulation of *Cdkn1a*, *Akt1* and the ERK pathway, causing placental growth arrest

Neha Sharma[1], Caroline Kubaczka[1], Stephanie Kaiser[2], Daniel Nettersheim[1], Sadaf S. Mughal[3], Stefanie Riesenberg[4], Michael Hölzel[4], Elke Winterhager[2] and Hubert Schorle[1,*]

ABSTRACT

Loss of TFAP2C in mouse leads to developmental defects in the extra-embryonic compartment with lethality at embryonic day (E)7.5. To investigate the requirement of TFAP2C in later placental development, deletion of TFAP2C was induced throughout extra-embryonic ectoderm at E6.5, leading to severe placental abnormalities caused by reduced trophoblast population and resulting in embryonic retardation by E8.5. Deletion of TFAP2C in TPBPA^{+} progenitors at E8.5 results in growth arrest of the junctional zone. TFAP2C regulates its target genes *Cdkn1a* (previously *p21*) and *Dusp6*, which are involved in repression of MAPK signaling. Loss of TFAP2C reduces activation of ERK1/2 in the placenta. Downregulation of *Akt1* and reduced activation of phosphorylated AKT in the mutant placenta are accompanied by impaired glycogen synthesis. Loss of TFAP2C led to upregulation of imprinted gene *H19* and downregulation of *Slc38a4* and *Ascl2*. The placental insufficiency post E16.5 causes fetal growth restriction, with 19% lighter mutant pups. Knockdown of *TFAP2C* in human trophoblast choriocarcinoma JAr cells inhibited MAPK and AKT signaling. Thus, we present a model where TFAP2C in trophoblasts controls proliferation by repressing *Cdkn1a* and activating the MAPK pathway, further supporting differentiation of glycogen cells by activating the AKT pathway.

KEY WORDS: TFAP2C, Trophoblast, Placenta, TPBPA, Junctional zone, MAPK

INTRODUCTION

In mice, the trophectoderm (TE) cells next to the inner cell mass form diploid extra-embryonic ectoderm (ExE) and ectoplacental cone (EPC), which further forms all trophoblast cells within the developing placenta (Rossant and Cross, 2001). Around E8.5, a subset of cells within EPC starts to express the gene *Tpbpa* (trophoblast-specific protein α) and differentiate into the junctional zone (JZ) of the placenta (Carney et al., 1993; Lescisin et al., 1988; Simmons et al., 2007). The JZ comprises spongiotrophoblast cells (SpTs) and glycogen trophoblast cells (GCs) interspersed by several blood canals lined by trophoblast giant cells (TGCs) called canal TGCs (C-TGCs) and the channel TGCs (Ch-TGCs) (Adamson et al., 2002; Gasperowicz et al., 2013; Guillemot et al., 1994). Aside from forming SpT and GCs, TPBPA^{+} cells give rise to all spiral artery-associated TGCs (SpA-TGCs) and half of C-TGCs (Simmons et al., 2007). The labyrinth, which comprises a dense network of fetal and maternal blood vessels lined by sinusoidal TGCs (S-TGCs) and syncytiotrophoblasts, is formed by the precursor cells within the chorion of the placenta (Cross et al., 2003). Labyrinth development is initiated by embryonic day (E)7.5 when a small cluster of cells within the chorion starts to express *Gcm1* (glial cells missing-1), which initiates branching morphogenesis (Anson-Cartwright et al., 2000).

Controlled proliferation and differentiation of trophoblast progenitor cells is essential for placental development. In humans, aberrant trophoblast differentiation leading to placental insufficiency is implicated in several disorders such as miscarriage, pre-eclampsia and intrauterine growth restriction (IUGR) (Kingdom et al., 2000). The transcription factor AP-2γ (TFAP2C) belongs to the activator protein-2 (AP-2) family (Eckert et al., 2005). In mice, *Tfap2c* expression is first detected in oocytes and all through preimplantation development (Auman et al., 2002; Cao et al., 2015; Choi et al., 2012; Kuckenberg et al., 2010). In mouse preimplantation embryo, *Tfap2c* has been recently demonstrated to be one of the first expressed trophoblast transcriptional regulators involved in trophoblast specification (Cao et al., 2015). At the blastocyst stage, TFAP2C is mainly detected in TE (Kuckenberg et al., 2010). Upon TE differentiation, TFAP2C protein is found in all trophoblast derivatives. Furthermore, during placental development, TFAP2C is present in SpT, GCs and TGCs including mononuclear S-TGCs that line the maternal sinusoids, but absent in syncytiotrophoblasts (Kuckenberg et al., 2010). In humans, TFAP2C is present in all trophoblast derivatives including extravillous trophoblasts, cytotrophoblasts and syncytiotrophoblasts (Kuckenberg et al., 2012). Its major site of expression is detected in the cytotrophoblast precursor cells, which give rise to the syncytiotrophoblasts (Biadasiewicz et al., 2011). Of note, increased levels of TFAP2C have been reported in pre-eclamptic placentae (Kotani et al., 2009).

Tfap2c-deficient mice die around E7.5 as a result of a defect in the developing ExE (Auman et al., 2002; Werling and Schorle, 2002). *Tfap2c* has been implicated in the specification and maintenance of trophoblast stem cell (TSC) fate (Kuckenberg et al., 2010; Werling and Schorle, 2002). Genome-wide chromatin immunoprecipitation in TSCs revealed that TFAP2C governs a set of genes involved in TSC self-renewal (Kidder and Palmer, 2010). Although these data emphasize the requirement of TFAP2C in the maintenance of the progenitor state of TE cells, the role of TFAP2C in the differentiating trophoblast is not understood. To examine the effect of loss of TFAP2C in the committed precursor

[1]Department of Developmental Pathology, Institute of Pathology, University of Bonn Medical School, 53127 Bonn, Germany. [2]Institute of Molecular Biology, University of Duisburg-Essen, University Clinics, 45211 Essen, Germany. [3]Division of Applied Bioinformatics, German Cancer Research Center (DKFZ), 69120 Heidelberg, Germany. [4]Unit for RNA Biology, Institute for Clinical Chemistry and Clinical Pharmacology, University Hospital Bonn, 53105 Bonn, Germany.

*Author for correspondence (Hubert.Schorle@ukb.uni-bonn.de)

Received 16 July 2015; Accepted 14 January 2016

Development (2016) 143, 787-798 doi:10.1242/dev.128553

lineages, we used a conditional mouse model to ablate TFAP2C in trophoblast precursor cells at E6.5 and E8.5, respectively. Loss of TFAP2C in ExE at E6.5 leads to a reduced number of trophoblasts resulting in embryonic retardation at E8.5. Loss of TFAP2C in TPBPA$^+$ precursor cells arrests the growth of the developing JZ. Downregulation of *Akt1* and reduced activation of AKT in the placenta upon loss of TFAP2C inhibits glycogen synthesis. Microarray analysis revealed upregulation of *Cdkn1a* (previously *p21*) and several dual-specificity phosphatases such as *Dusp1*, *Dusp4* and *Dusp6*, which are repressors of mitogen activated protein kinase (MAPK) signaling. TFAP2C binds to the promoter of *Cdkn1a* and *Dusp6*, thereby directly regulating the expression of these target genes. The reduced activation of MAPK (pERK1/2, pP38) and AKT pathways upon loss of TFAP2C was further validated in the human choriocarcinoma cell line (JAr). JAr cells represent human trophoblasts and cytotrophoblast cells *in vitro* in terms of morphology and hormone production (Aladjem and Lueck, 1981; Pattillo et al., 1971). Furthermore, the cells of cytotrophoblast columns in human placenta are analogous to the EPC in mouse, which differentiate into giant cells (Rossant and Cross, 2001). These results suggest that, in trophoblasts, TFAP2C represses *Cdkn1a* and negative regulators of the MAPK pathway (*Dusp1*, *Dusp4* and *Dusp6*). TFAP2C is also required for activating the AKT pathway, which is involved in glycogen synthesis.

RESULTS

Loss of TFAP2C within the ExE post E6.5 exhibits severe placental defects

To study requirement of TFAP2C in early placental development, we took advantage of a mouse model expressing Cre recombinase under the bovine K5 promoter active in early embryogenesis at E6.5 in the ExE (Crish et al., 2013; Ramirez et al., 2004) and crossed it with a mouse harboring a floxed *Tfap2c* allele (*Tfap2c*$^{fl/fl}$) (Werling and Schorle, 2002) to generate *K5Cre:Tfap2c*$^{-/-}$ embryos. At E7.5, IHC showed loss of TFAP2C protein in the cells of ExE and EPC in the *K5Cre:Tfap2c*$^{-/-}$ embryos but not in wild-type or heterozygous embryos (herein referred to as control) indicative of efficient loss of TFAP2C (Fig. S1A). *K5Cre:Tfap2c*$^{-/-}$ implantations were considerably smaller than controls suggesting a developmental retardation of the embryo (Fig. S1B,C). Hematoxylin and Eosin (H/E)-stained sections revealed no formation of JZ and labyrinth in mutant placentae (Fig. 1A, H/E). Furthermore, in *K5Cre:Tfap2c*$^{-/-}$ placentae, the region where the SpT are localized comprised loosely arranged TGCs interspersed by maternal blood (Fig. 1A, H/E, arrowheads). The number of Ki-67$^+$ proliferating cells was severely reduced in the mutant placentae (Fig. 1A, Ki-67). The labyrinth of control placentae contained CD31$^+$ fetal endothelial blood vessels comprising primitive nucleated fetal blood cells. Interestingly, the mutant placentae showed very few and small fetal endothelial vessels with no fetal blood (Fig. 1A, CD31) suggesting that labyrinth formation was initiated but severely impaired. *In situ* hybridization (ISH) revealed reduced expression of *Prl3d1* (also known as *PL1*), which is a marker of parietal-TGCs (P-TGCs) and *Prl2c2*, a marker of SpA-TGCs in *K5Cre:Tfap2c*$^{-/-}$ placentae (Fig. 1B). Also, *Prl2c2*-expressing SpA-TGCs within the mutant placentae showed poor invasion of maternal blood vessels compared with the controls (Fig. 1B, Prl2c2). The number of *Tpbpa*$^+$ SpT cells was markedly reduced and displayed reduced invasion into the decidua (Fig. 1B, Tpbpa). Next, gene expression analysis of E8.5 whole placentae (n=4 each) showed a significant downregulation of the progenitor markers *Tpbpa* (P=0.009) and *Gcm1* (P=0.032), the differentiation markers *Prl3d1* (P=0.006), *Prl2c2* (P=0.012) and *Hand1* (P=0.007), which are important for TGC differentiation (Hemberger et al., 2004) and *Ascl2* (P=0.029), which is required for the maintenance of JZ (Tanaka et al., 1997) (Fig. 1C). Thus, loss of TFAP2C in early placental morphogenesis most likely affects the trophoblast stem cell/progenitor compartment, leading to a general reduction of all trophoblast subtypes.

Loss of TFAP2C in TPBPA$^+$ precursor cells leads to a growth arrest of the JZ

To investigate the loss of TFAP2C in the TPBPA$^+$ progenitor cells, *Tpbpa-Cre* mice (Simmons et al., 2007) were mated with *Tfap2c*$^{fl/fl}$ mice (Werling and Schorle, 2002). IHC confirmed loss of TFAP2C in JZ of *TpbpaCre:Tfap2c*$^{-/-}$ placentae at E14.5 (Fig. 2A). The JZ was extracted using laser microdissection and RNA was isolated (n=4 each). Here, the level of *Tfap2c* expression was significantly reduced in the JZ of *TpbpaCre:Tfap2c*$^{-/-}$ placentae (P<0.0001, Fig. 2B) further validating the loss of *Tfap2c* in TPBPA$^+$ cells. The remaining level of *Tfap2c* expression might emanate from TPBPA-negative cells within the JZ or might be due to incomplete excision of the *Tfap2c* allele in TPBPA-positive cells (Fig. 2B). Next, we observed that the JZ did not further increase in area from E12.5 onwards in the mutant placentae (Fig. 2C). Morphometric analyses demonstrated that the JZ area was comparable in size at E10.5 but significantly retarded in development at E12.5 (n=3 each, P=0.02), resulting in only 50% of the area of wild-type JZ at E14.5 (n=6 each; P=0.007), 75% at E16.5 (n=4 each; P<0.0001) and 80% at E18.5, respectively (n=6 each; P<0.0001; Fig. 2D). However, the overall area of mutant placentae displayed only a non-significant reduction from E14.5 onwards (Fig. S2A). Because we detected a slight increase in the labyrinth area in the mutant placentae at E16.5 and E18.5, we speculate that the growth impairment of the JZ might be compensated by the increase in labyrinth (Fig. S2B). Despite this, the mutant placentae at E16.5 (P=0.01, n=11 control, n=3 mutant) and E18.5 (P=0.0006, n=13 control, n=7 mutant), were significantly lighter compared with the controls (Fig. S2C). The labyrinth of mutant placentae displayed no gross morphological defect and the number of CD31$^+$ fetal endothelial vessels within the labyrinth did not change (Fig. S2D). We next found a reduced number of Ki-67$^+$ proliferating cells in mutant placentae from E10.5 onwards (Fig. 2E). Quantitative estimation revealed that in mutant placentae at E10.5, 51.87% (P=0.017) and at E12.5 (P=0.0009) only 25.47% of cells were Ki-67$^+$ compared with the control (set as 100%) (Fig. 2F). TUNEL assay at E12.5 did not reveal any apoptotic cells in the control and mutant placentae (Fig. S2E). This result strongly suggests that the growth arrest seen in TFAP2C negative JZ is due to a lack of proliferation and not enhanced apoptosis.

Loss of TFAP2C in TPBPA$^+$ cells affects trophoblast subtypes and impairs GC differentiation

To further characterize trophoblast subtypes affected, we performed ISH and found reduced numbers of *Tpbpa*-expressing cells in the mutant placentae from E12.5 onwards. *Tpbpa*-expressing cells were scarcely scattered in the JZ at E14.5 and completely absent from E16.5 onwards (Fig. 3A). This suggested that TFAP2C is required to maintain *Tpbpa* expression in these cells. Furthermore, *Prl2c2*$^+$ SpA-TGCs invading the maternal arteries and *Prl3b1*$^+$ C-TGCs were both reduced in the mutant placentae (Fig. 3B,C). The number of P-TGCs at E12.5 placental sections (n=3 each) in the control and mutant placenta was not altered (Fig. S3A). From E11.5, the GCs

Development (2016) 143, 787-798 doi:10.1242/dev.128553

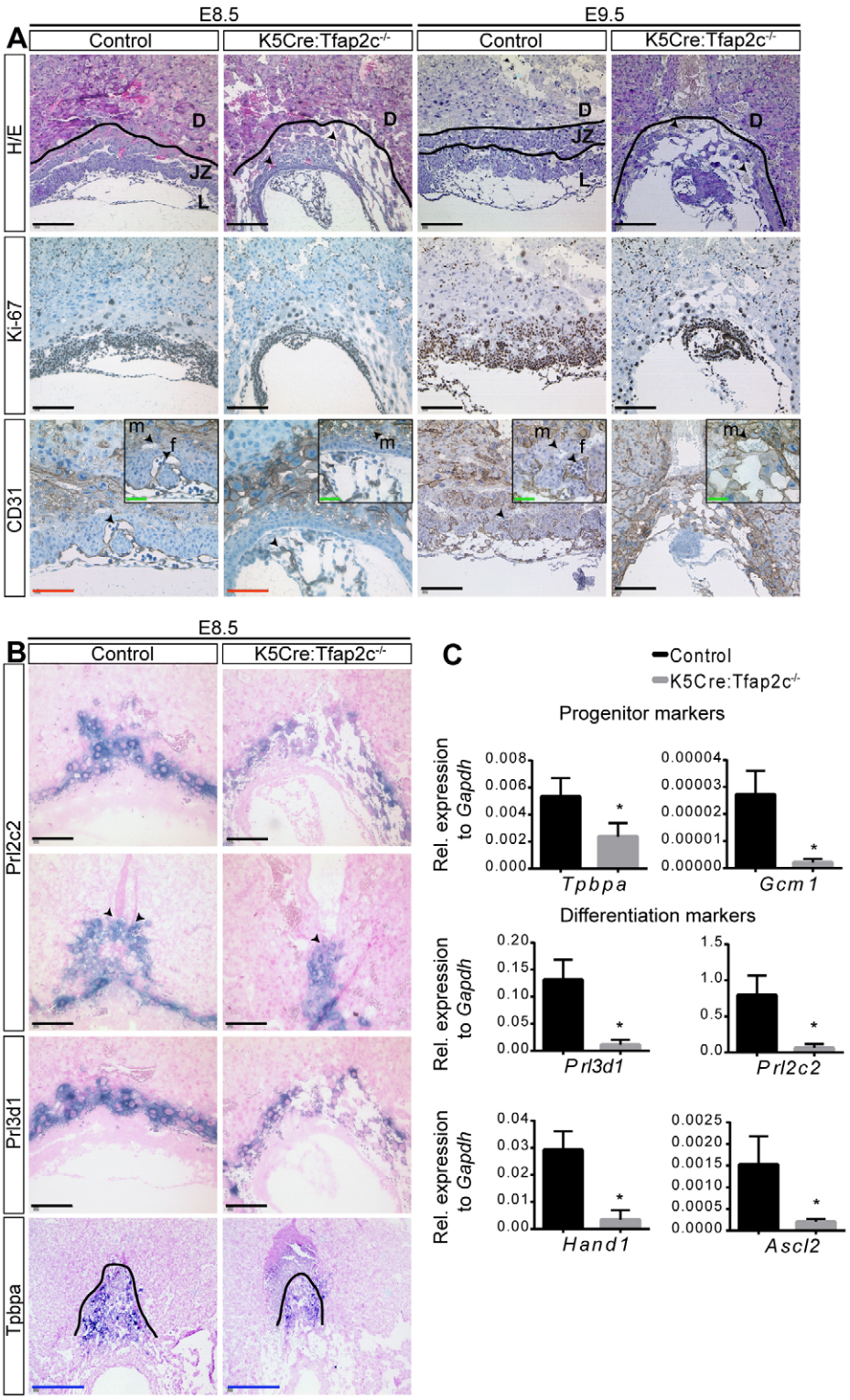

Fig. 1. Loss of TFAP2C within ExE results in severe morphological alterations in the placenta. (A) Control and *K5Cre:Tfap2c*$^{-/-}$ placentae at E8.5 (n=3 each) and E9.5 (n=2 *K5Cre:Tfap2c*$^{-/-}$; n=3 control) stained with hematoxylin and eosin (H/E). The *K5Cre:Tfap2c*$^{-/-}$ placentae were severely impaired, with no formation of JZ or labyrinth. Arrows indicate TGCs interspersed in decidual sinusoids. Ki-67 IHC shows reduced number of proliferating cells in *K5Cre:Tfap2c*$^{-/-}$ placentae. There is a reduced number of CD31^{+} fetal vessels in *K5Cre:Tfap2c*$^{-/-}$ placentae. Boxed image at higher magnification reveals presence of fetal and maternal blood in control but not in *K5Cre:Tfap2c*$^{-/-}$ placentae, as indicated by arrows. (B) ISH showing reduced number of TGCs expressing *Prl2c2*. Number of P-TGCs expressing *Prl3d1* and SpT cells expressing *Tpbpa* decrease in *K5Cre:Tfap2c* $^{-/-}$ placentae. (C) Expression levels of trophoblast markers relative to *Gapdh* by qRT-PCR on implantations from E8.5. All trophoblast markers are downregulated in *K5Cre:Tfap2c*$^{-/-}$ compared with the control. Data are represented as means±s.d., *P≤0.05 (Student's t-test). m, maternal blood; f, fetal blood; JZ, junctional zone; D, deciduas; L, labyrinth. Scale bars: black, 200 µm; red, 100 µm; green, 50 µm and blue, 500 µm.

start to accumulate glycogen in their cytoplasm and increase in size and are characterized as vacuolated terminally differentiated GCs (Coan et al., 2006). Morphologically, GCs in mutant placentae were much smaller, with only weak accumulation of glycogen and were not as strongly vacuolated, suggesting that they are not terminally differentiated (Fig. 3D). Next, we detected 25% reduction of glycogen in the mutant placentae (P=0.0418) at E14.5 (n=5 mutant; n=9 control; Fig. 3E). Thus, loss of TFAP2C affects all trophoblasts derived from the TPBPA^{+} population.

Deficit of endocrine hormones is indicative of a reduced trophoblast population within JZ

We next performed an expression microarray analysis (Illumina Mouse WG-6 v2.0). Because microdissection of JZ yields little RNA, samples from TFAP2C mutant (n=3) and control placentae (n=3) at E13.5 were pooled to perform the analysis. A scatter plot revealed that in mutant placentae 146 genes were upregulated and 51 genes were downregulated significantly with fold change ≥1.5 in $\log_2$ scale compared with the control (Fig. 4A). Deregulated genes

Development (2016) 143, 787-798 doi:10.1242/dev.128553

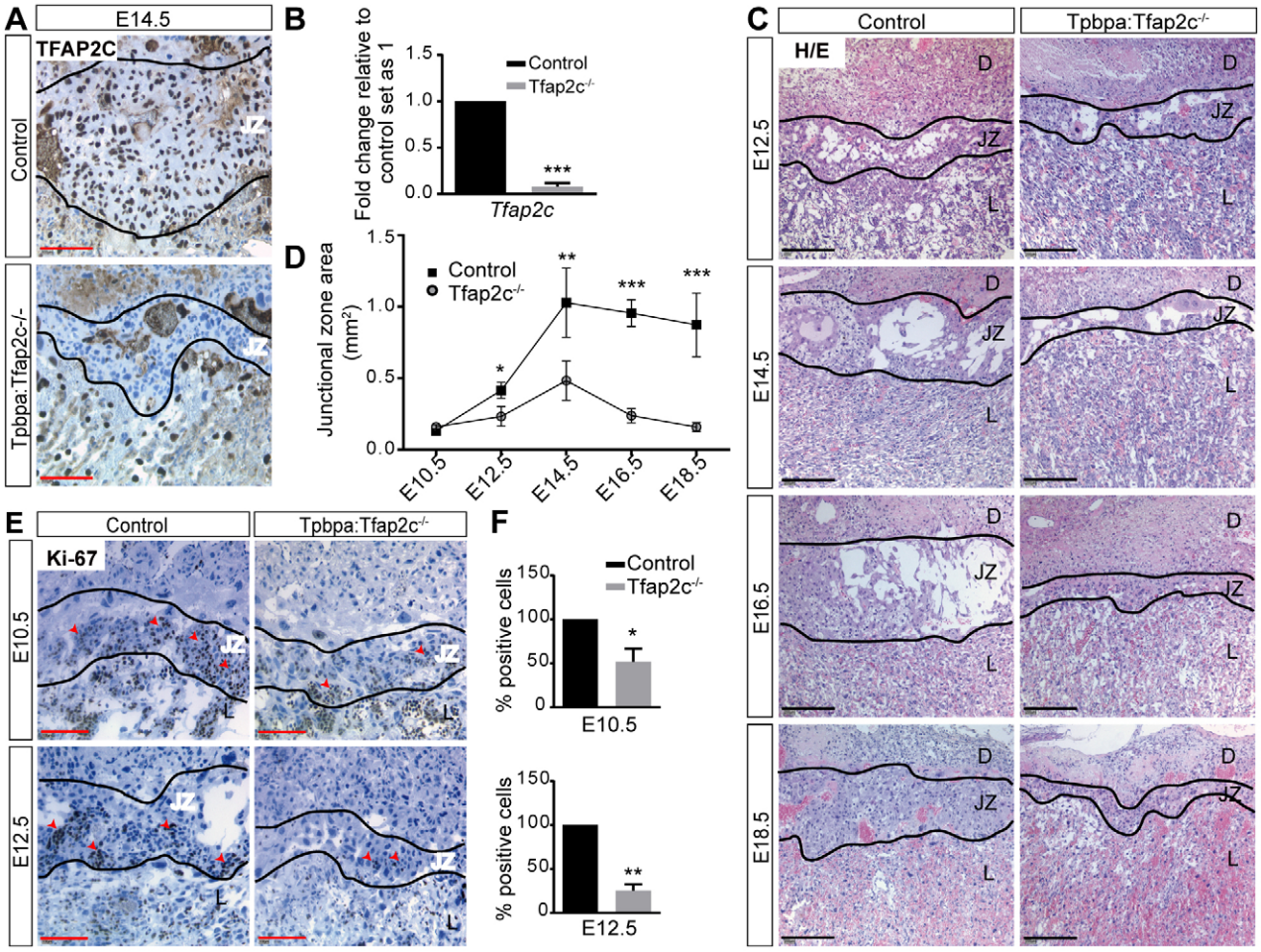

Fig. 2. Loss of TFAP2C in TPBPA-positive precursor cells leads to a growth arrest of the JZ. (A) IHC depicting loss of TFAP2C protein within the JZ of *Tpbpa:Tfap2c*$^{-/-}$ placentae at E14.5. (B) Samples obtained by laser microdissection of SpT from E14.5 *Tpbpa:Tfap2c*$^{-/-}$ and control placentae (n=4 each) showing significantly reduced level of *Tfap2c* in *Tpbpa:Tfap2c*$^{-/-}$ placentae. (C) H/E staining on sections from E12.5 to E18.5 shows growth arrest of JZ in *Tpbpa:Tfap2c*$^{-/-}$ placentae compared with the control. (D) JZ area of *Tpbpa:Tfap2c*$^{-/-}$ placentae at E10.5 (n=3 control, n=2 mutant), E12.5 (n=3 each), E14.5 (n=6 each), E16.5 (n=4 each) and E18.5 (n=6 each) was significantly reduced compared with control placentae. (E) Arrowheads indicate reduced number of Ki-67^{+} cells at E10.5 and E12.5 in JZ of *Tpbpa:Tfap2c*$^{-/-}$ placentae. (F) Percentage of proliferating cells in *Tpbpa:Tfap2c*$^{-/-}$ placentae (n=3 images from different sections) was significantly reduced at both E10.5 and E12.5. Scale bars: black, 200 µm; red, 100 µm. All data are represented as means±s.d. ***P≤0.0005, **P≤0.005, *P≤0.05 (Student's t-test). JZ, junctional zone; D, deciduas; L, labyrinth.

are summarized in Tables S1 and S2 and a heat map depicting differential expression of deregulated genes is shown in Fig. S4A. Deregulated genes were categorized according to Gene Ontology into several groups (Table S3). Selected genes were further analyzed and are represented in the form of a heat map (Fig. 4B). The pregnancy-specific glycoprotein (Psg) and carcinoembryonic antigen-related adhesion molecules (CEACAMs) are synthesized by the TGCs and SpT cells in the mouse placenta (Kromer et al., 1996; Wynne et al., 2006; Zhou et al., 1997). Interestingly, many of the downregulated genes in the mutant placentae belong to the CEA family (*Psg18*, *Psg22*, *Psg23*, *Ceacam13*, *Ceacam14*, *Ceacam3*) and prolactin-associated protein family (*Prl4a1*, *Prl3c1*, *Prl7c1*, *Prlpc3*) (Fig. 4B). Additionally, we found upregulation of genes involved in vasculogenesis and angiogenesis (*Vegfa*, *Pdgfa*) (Arroyo and Winn, 2008; Mayhew et al., 2004). Genes representative for the different categories were further validated by qRT-PCR. *Psg18* was significantly reduced (P=0.0022; Fig. S4B), whereas *Vegfa* was upregulated more than 3-fold in the mutant placentae (P=0.046; Fig. S4C). We confirmed downregulation of several endocrine hormones synthesized by different trophoblast population at E14.5 by qRT-PCR (n=4 each; Fig. 4C). *Gjb3*, a marker of differentiated GCs (Coan et al., 2006) was also reduced in the mutant placentae validating our finding that the GCs in the mutant placentae do not accumulate sufficient glycogen (Fig. 4C; fold changes and P values are summarized in Table S4). In line with this, we observed a significant reduction of *Akt1* expression in mutant placentae (P=0.0183; Fig. S4D). AKT1 is involved in PI3K-AKT-mediated synthesis of glycogen stores within GCs (Cross et al., 1995; Yang et al., 2003). To confirm loss of activated AKT in the placenta, we performed IHC on E14.5 placental sections and found a 3-fold reduction (P=0.0038) in the number of phospho-AKT (pAKT)-positive cells in the JZ of mutant placenta (Fig. S4E,F).

Ch-TGCs were not altered in the mutant placentae most probably because they are derived from a TPBPA-negative population (Fig. 4C). We did not find any significant changes in the expression levels of *Hand1* and *Cdkn1c* (*P57*), which are involved in TGC differentiation (Hemberger et al., 2004; Takahashi et al., 2000) (Fig. S3B) or the P-TGC marker *Prl3d1* (Fig. 4C). Expression levels of *Tfap2c* and *Gcm1* in the labyrinth

Development (2016) 143, 787-798 doi:10.1242/dev.128553

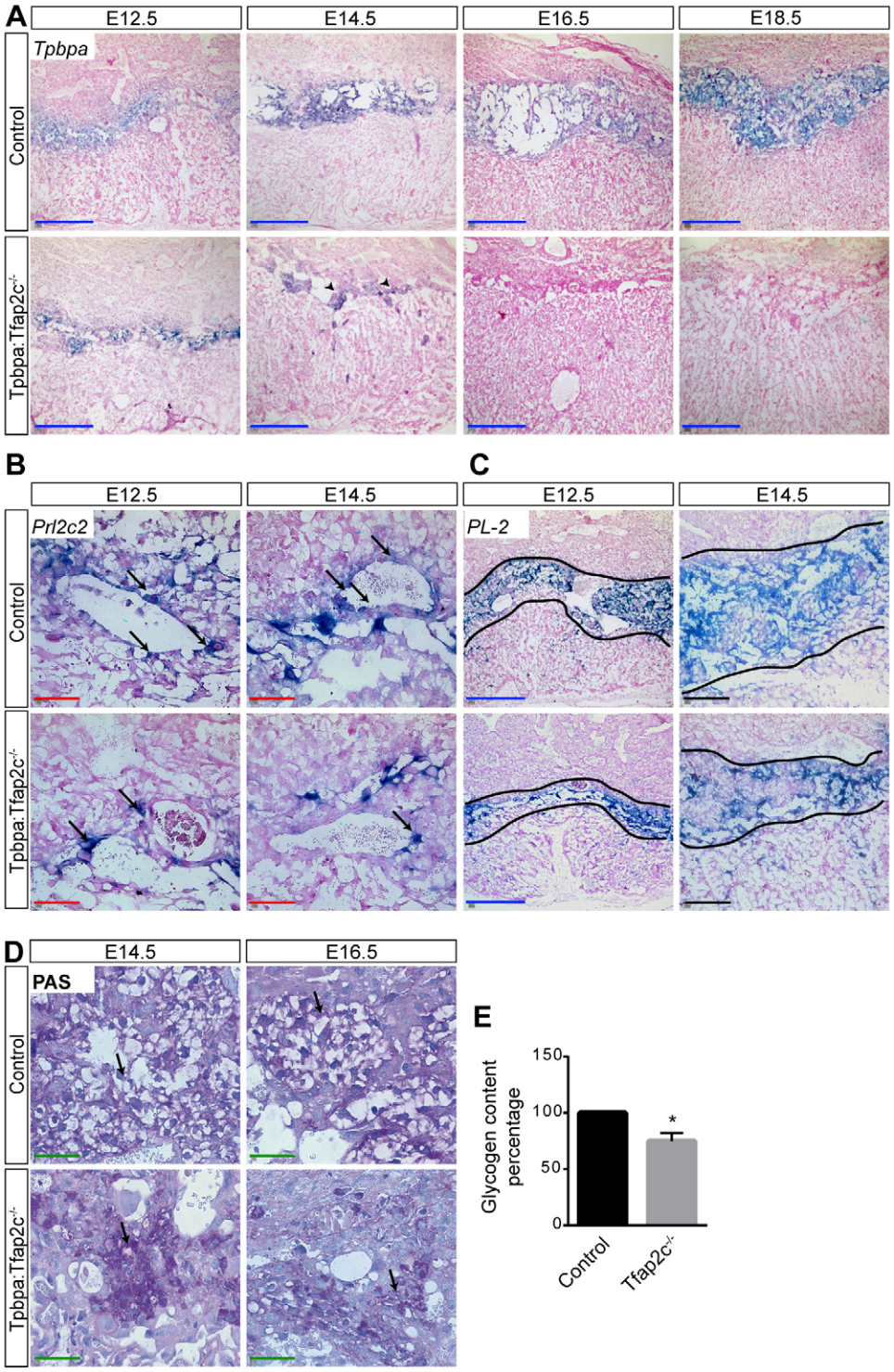

Fig. 3. Loss of TFAP2C in TPBPA precursor cells affects trophoblast subtypes and impairs GC differentiation. ISH for trophoblast markers *Tpbpa*, *Prl2c2* and *Prl3b1* (*Pl2*) was performed. (A) *Tpbpa*$^{+}$ cells were dramatically reduced from E12.5 onwards in *Tpbpa:Tfap2c*$^{-/-}$ placentae. (B) Arrows indicate reduced number of SpA-TGCs expressing *Prl2c2* in *Tpbpa:Tfap2c*$^{-/-}$ placentae at both E12.5 and E14.5. (C) TGC marker *Prl3b1* (*Pl2*) expression is also reduced in *Tpbpa:Tfap2c*$^{-/-}$ placentae compared with the control. (D) PAS reaction on sections reveals impaired differentiation of GCs in *Tpbpa:Tfap2c*$^{-/-}$ placentae. Arrows indicate terminally differentiated GCs in control placentae whereas GC islets in the *Tpbpa:Tfap2c*$^{-/-}$ placentae are not differentiated. (E) Glycogen extracted from whole placenta (n=9 control and n=5 *Tpbpa:Tfap2c*$^{-/-}$) was 25% reduced in *Tpbpa:Tfap2c*$^{-/-}$ placentae compared with the control set to 100%. Scale bars: black, 200 µm; red, 100 µm; blue, 500 µm; green, 50 µm. *$P \leq 0.05$ (Student's t-test).

were unaffected; however, the S-TGC markers *Prl2c2*, *Ctsq* and *Prl3b1* were slightly elevated in mutant placentae (Fig. S3C). Also, an increase in the number of *Prl3b1*-expressing S-TGCs was observed within the labyrinth of the mutant placenta (Fig. S3D).

Because imprinted genes are known to be crucial for placental development, we investigated expression of several imprinted genes and found significant upregulation of *H19* (P=0.03), downregulation of *Ascl2* (P=0.00054) and *Slc38a4* (P<0.0001) (Fig. 4C), whereas levels of *Phlda2* and *Igf2* were unaffected (Fig. S3E). Deregulation of imprinted genes suggested loss of imprinting. To check this further, we sought to analyze methylation status of the imprinted gene *H19*, which is known to act as a trans-regulator of imprinted gene network thereby controlling mouse embryonic growth. The *H19*/*Igf2* imprinted control region (ICR), which is located upstream of the *H19* promoter contains several differentially methylated regions (DMRs) including CCCTC binding factor (CTCF) binding sites which perform diverse regulatory functions such as transcriptional activation/repression and imprinting (Gabory et al., 2009; Phillips and Corces, 2009). We looked for the methylation pattern of 6 CpGs within a CTCF3

Development (2016) 143, 787-798 doi:10.1242/dev.128553

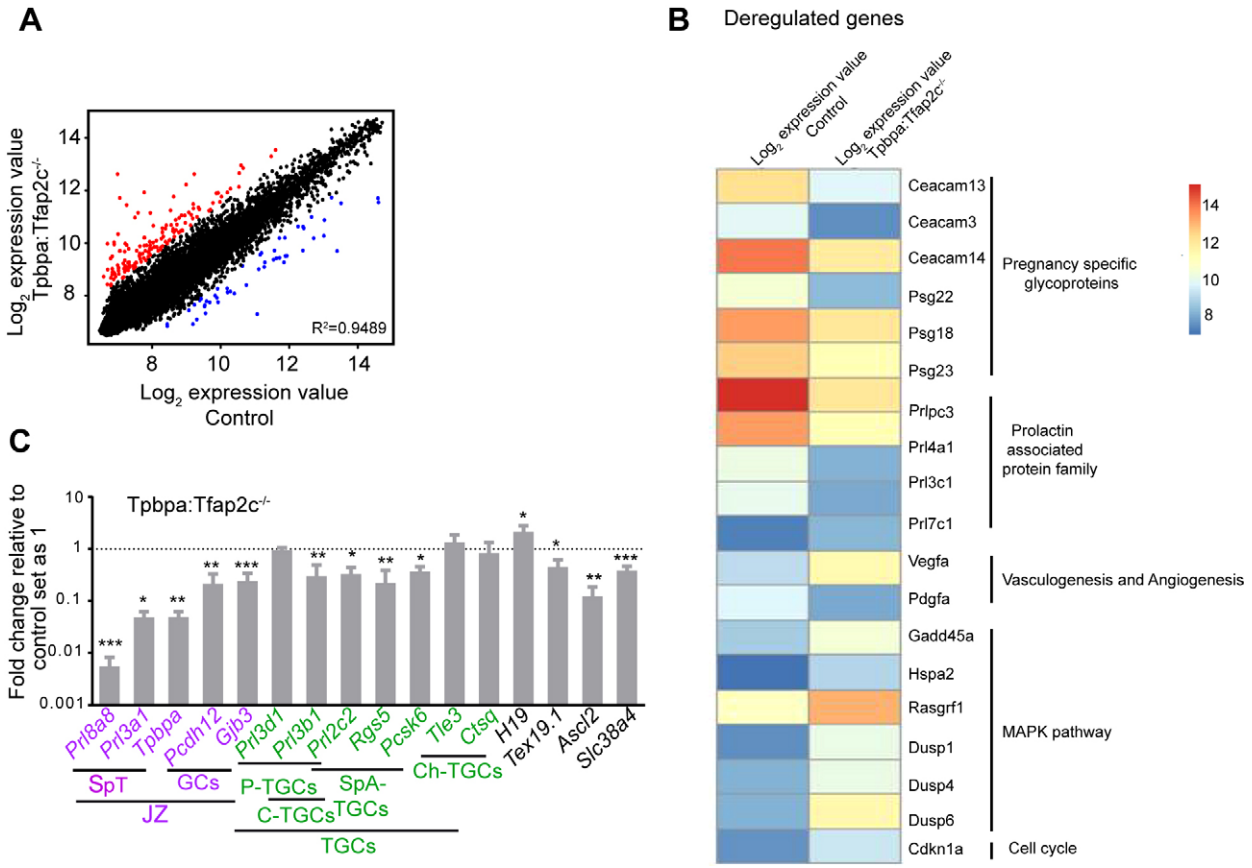

Fig. 4. Expression microarray analysis. (A) Scatter plot of global gene expression of laser microdissected JZ from control and *Tpbpa:Tfap2c*$^{-/-}$ placentae. Black dots indicate genes with fold change less than 1.5 in $\log_2$ scale. Upregulated genes are indicated in red and downregulated genes in blue compared with the control. *R*, Fisher's correlation coefficient. (B) Heat map showing expression values of selected deregulated genes in control and *Tpbpa:Tfap2c*$^{-/-}$ placentae with fold change ≥1.5 in $\log_2$ scale. Log-transformed expression values are presented on a scale of 8 to 14. Upregulated genes are indicated in shades of red; downregulated in blue. Genes synthesizing endocrine hormone belonging to pregnancy-specific glycoproteins and prolactin-associated proteins were downregulated. Genes involved in angiogenesis were upregulated. Genes belonging to MAPK signaling were differentially deregulated. The cell cycle regulator *Cdkn1a* was upregulated. (C) qRT-PCR analysis showing fold change expression of several trophoblast markers from laser microdissected samples of SpT from E14.5 *Tpbpa:Tfap2c*$^{-/-}$ and control placentae (n=4 each). Downregulation of endocrine hormones such as *Prl8a8*, *Prl3a1*, *Prl2c2*, *Prl3d1* (*Pl1*) and *Prl3b1* (*Pl2*) is indicative of reduced trophoblast population. ***P≤0.0005, **P≤0.005, *P≤0.05 (Student's t-test). Data are represented as means±s.d.

binding site using cells from the JZ of *Tfap2c* mutant and control placentae. We found no differential methylation (n=14 control, n=15 mutant; Fig. S4G), indicating that imprinting within this region is not affected upon loss of TFAP2C. Loss of TFAP2C also deregulated *Tex19.1* (P=0.03; Fig. 4C).

We further utilized GENEMANIA, a web-based tool prioritizing gene interaction based on the available genomics and proteomics data to find interactive gene networks between *Tfap2c* and deregulated genes (Fig. S5). *Tfap2c* was linked to several endocrine genes, suggesting coordinated expression of *Tfap2c* and these genes (Fig. S5A). Interestingly, we found co-expression of *Tfap2c* and *Tpbpa* (Fig. S5A), supporting our speculation that upon loss of *Tfap2c* expression, cells also downregulate expression of *Tpbpa* in the placenta. The deregulated genes were further subjected to analysis using STRING web-based tool to find known and predicted protein interactions between *Tfap2c* and deregulated genes (Fig. S5B).

Loss of *Tfap2c* expression leads to derepression of *Cdkn1a* and Dusp genes involved in the MAPK signaling pathway in mouse and human trophoblasts

We validated the upregulation of *Cdkn1a* by more than 3-fold (P=0.00018) in the JZ of the mutant placentae at E14.5 by qRT-PCR (Fig. 5A). Furthermore, several genes involved in repression of the MAPK signaling pathway (*Hspa2*, *Gadd45a*, *Dusp6*, *Rasgrf1*, *Dusp1*, *Pdgfa*, *Dusp4*, *Fos*; Table S3; Keyse, 2008) were deregulated (Fig. 4B). *Dusp1*, *Dusp4* and *Dusp6* were further validated by qRT-PCR and were significantly upregulated (P=0.00058, P=0.00804, P=0.0182, respectively) upon loss of TFAP2C in the JZ (Fig. 5B). These data demonstrated that TFAP2C represses *Cdkn1a* and negative regulators of MAPK signaling. Thus, we hypothesized that the MAPK pathway is downregulated in the mutant placentae. To further verify our findings, we analyzed phospho-ERK1/2 (pERK1/2) signal in the JZ at E14.5 (Fig. 5C). On average, 3.2% of cells within the JZ were positive for pERK1/2 in the mutant placentae (n=3) compared with 7.5% positive cells in the control placentae (n=2) (Fig. 5D). Because loss of TFAP2C reduced the activation of ERK1/2 at E14.5, we asked whether the levels of ERK1/2 activation would also be compromised at E7.5 upon loss of TFAP2C in ExE and EPC. IHC at E7.5 showed absence of pERK1/2 signal in the mutant embryos (Fig. S1A). Hence, TFAP2C modulates MAPK signaling in the murine placenta. We next asked whether TFAP2C is able to directly regulate cell proliferation and MAPK signaling by binding to promoter regions of *Cdkn1a* and *Dusp6*. To this end, we performed ChIP analysis utilizing trophoblast stem cell TS-6.5 (Kubaczka et al., 2014), differentiated for 5 days as a corollary for placenta. Information

Development (2016) 143, 787-798 doi:10.1242/dev.128553

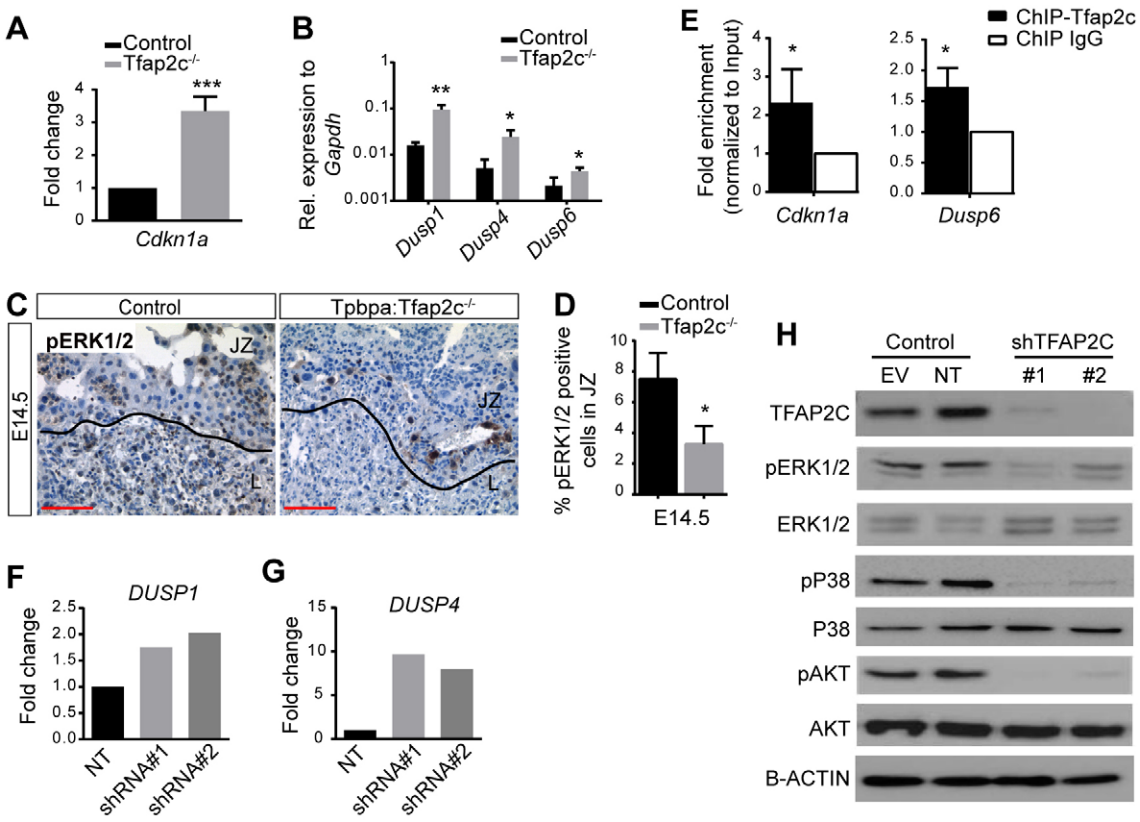

Fig. 5. Loss of TFAP2C leads to derepression of *Cdkn1a* and Dusp genes involved in the MAPK signaling pathway in mouse and human trophoblasts. (A) qRT-PCR showing fold change expression of *Cdkn1a* in *Tpbpa:Tfap2c*$^{-/-}$ SpT relative to control (n=4 each). (B) qRT-PCR showing relative expression of *Dusp1*, *Dusp4* and *Dusp6*. (C) pERK1/2 IHC on E14.5 placental sections. Scale bars: 100 µm. (D) Quantification of pERK1/2-positive cells in the JZ of placenta (n=3 each genotype). (E) q-PCR following ChIP analysis showing enrichment of TFAP2C to the promoter region of *Cdkn1a* and *Dusp6* normalized to 2% input samples in day 5 differentiated trophoblast cells. qRT-PCR showing fold change upregulation of (F) *DUSP1* and (G) *DUSP4* in two independent TFAP2C-knockdown constructs compared with non-targeted control (NT). (H) Western blot depicting knockdown of TFAP2C in JAr cells using two different shRNA constructs (#1 and #2) together with empty vector (EV) and NT controls. Loss of TFAP2C reduces activation of MAPK pathway (pERK1/2, pP38) and pAKT. ***P≤0.0005, **P≤0.005, *P≤0.05 (Student's t-test).

about TFAP2C binding sites in the promoter region of *Cdkn1a* were taken from Schemmer et al. (2013) and the binding site in the *Dusp6* promoter region was identified by the rVista algorithm. Both were enriched for TFAP2C (*Cdkn1a*, 2.3×, P=0.045; *Dusp6*, 1.7×, P=0.032), implicating both as direct targets of TFAP2C (Fig. 5E).

To further validate that MAPK and AKT signaling pathways are indeed compromised upon loss of TFAP2C, we utilized the human choriocarcinoma JAr cells as a human trophoblast model system (White et al., 1988). JAr cells were transduced with two independent shRNA knockdown constructs targeting TFAP2C and analyzed thereafter. As in murine placenta, expression levels of *DUSP1* and *DUSP4* were upregulated upon loss of TFAP2C (Fig. 5F,G). Western blot analysis demonstrated that transduction of both shRNA knockdown constructs resulted in a high reduction of TFAP2C protein (Fig. 5H). Downregulation of TFAP2C, led to a dramatic reduction in pERK1/2 and phosphorylated P38 (MAPK14), whereas the total levels of ERK and P38 remained constant (Fig. 5H). Furthermore, upon loss of TFAP2C, AKT signaling was also inhibited (Fig. 5H). Taken together, loss of TFAP2C leads to a downregulation of AKT and MAPK signaling in murine, as well as human trophoblast models.

JZ TFAP2C-deprived embryos are growth restricted

Given that TFAP2C-deprived JZ in the mutant placentae displays morphological defects from E12.5 onwards with a severely compromised JZ by E14.5 and altered expression of several trophoblast subtypes, we weighed embryos post E14.5 and found that the fetal mass at E16.5 (P<0.0001, n=11 control and n=3 mutant) and E18.5 (P<0.0001, n=13 control and n=7 mutant) was significantly reduced (Fig. 6A). The mutant embryos were approximately 19% lighter from E16.5 onwards and maintained the lower mass until term. After birth, the mutant pups were 17% lighter in the first week and 10% lighter in the second and third week, respectively (n=39 control, n=11 mutant; Fig. 6B). Following weaning, the mass of mutant animals caught up and remained comparable to the mass of the controls. Fig. 6C shows mutant pups at E18.5, postnatal day 4 and 14, respectively. Thus, placental insufficiency caused by loss of TFAP2C within the JZ leads to a fetal growth restriction post E16.5, which is overcome after birth.

DISCUSSION

We demonstrate that the loss of TFAP2C in the stem/progenitor compartment of the ExE leads to a severe placental malformation with strikingly reduced numbers of trophoblasts. Loss of TFAP2C in TPBPA^{+} cells arrests the development of JZ, affecting TPBPA-derived trophoblasts. Upregulation of *Cdkn1a* and downregulation of *Akt1* upon loss of TFAP2C is indicative of imbalance between proliferation of trophoblasts and differentiation of GCs leading to 75% smaller JZ. Furthermore, TFAP2C represses *Dusp1*, *Dusp4* and *Dusp6*, which are involved in repressing MAPK signaling. We

Development (2016) 143, 787-798 doi:10.1242/dev.128553

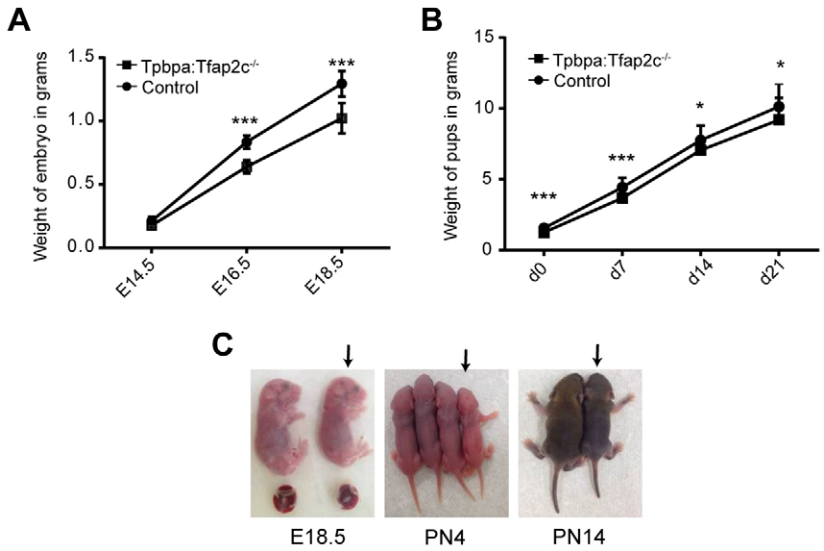

Fig. 6. JZ TFAP2C-deprived embryos are growth restricted. (A) Mass of embryos at E14.5 (n=18 control, n=4 mutant), E16.5 (n=11 control, n=3 mutant) and E18.5 (n=13 control, n=7 mutant). (B) Mean mass of newborn pups from *Tpbpa:Tfap2c*$^{-/-}$ and control placenta until day 21. The mutant pups (n=11) are significantly lighter than the control (n=39) pups. ***P≤0.0005, *P≤0.05 (Student's t-test). Data are represented as means±s.d. (C) Image depicting lighter *Tpbpa:Tfap2c*$^{-/-}$ placentae and embryos at E18.5, PN4 (postnatal day 4) and PN14 (postnatal day 14), respectively. Arrows indicate mutant pups derived from *Tpbpa:Tfap2c*$^{-/-}$ placentae.

observed reduced ERK1/2 activation upon loss of TFAP2C in the JZ of placenta. This is achieved by direct regulation of *Cdkn1a* and *Dusp6* by TFAP2C. Knockdown of TFAP2C in JAr cells confirms reduced activation of the MAPK (ERK1/2 and P38) and AKT signaling pathways.

Choi et al. demonstrated increased *Cdkn1a* expression in TFAP2C-deficient preimplantation embryos, resulting in growth arrest at morula stage, which could be rescued by RNAi-mediated depletion of *Cdkn1a* (Choi et al., 2012). In line with this, we show that loss of TFAP2C in the JZ leads to upregulation of *Cdkn1a* and consequently growth arrest. The MAPK signaling pathway has been demonstrated to be essential in trophoblast differentiation. Although expression of *ERK1/2* (*MAPK3* and *MAPK1*) in the human villous cytotrophoblast cells but not in the syncytiotrophoblasts has been observed throughout pregnancy, activated ERK1/2 in the villous cytotrophoblast cells is detected up to 12 weeks of gestation (Kita et al., 2003). The presence of activated ERK1/2 within the committed cytotrophoblast progenitors both in human placenta and primary trophoblast culture suggests that activation of the MAPK pathway is important for initiation of trophoblast differentiation (Daoud et al., 2005). In mice, disruption of the *Erk2* gene leads to embryonic lethality due to failure in formation of EPC and ExE (Saba-El-Leil et al., 2003). Also, knockdown of TFAP2C reduces activation of the ERK1/2 pathway in MCF-7 cells (Spanheimer et al., 2014). Thus, TFAP2C stimulates the MAPK signaling pathway in different cell types. TFAP2C does seem to directly affect proliferation and MAPK signaling in differentiated trophoblast by binding to the promoter of its targets, *Cdkn1a* and *Dusp6*, which are involved in repressing MAPK signaling. In 2010, Kidder and Palmer showed that promoters of several Dusp genes are bound by TFAP2C in murine TSCs (Kidder and Palmer, 2010). Loss of TFAP2C in murine placenta, as well as in JAr cells, leads to upregulation of DUSPs, suggesting that TFAP2C seems to regulate MAPK activity by suppressing levels of DUSPs.

Akt1 is involved in placental development and fetal growth in mice because *Akt1*$^{-/-}$ placenta shows a complete loss of GCs causing placental dysfunction and growth retardation of the fetus (Yang et al., 2003). Furthermore, *Prl2*$^{-/-}$ (phosphatase of regenerating liver 2) placenta also displays reduced activation of AKT, leading to inhibition of glycogen synthesis (Dong et al., 2012). Mechanistically, pAKT inhibits GSK3B, which leads to glycogen synthesis (Cross et al., 1995; Diehl et al., 1998). Thus, the reduced expression of *Akt1* and reduced activation of AKT observed upon loss of TFAP2C leads to a decrease in glycogen stores.

Does apoptosis contribute to the growth arrest of the JZ? Ablation of TPBPA^{+} cells with diptheria toxin led to an embryonic lethality at E11.5 (Hu and Cross, 2011). If, upon loss of TFAP2C, the cells within the JZ were to undergo apoptosis, it should have resembled a phenocopy of the TPBPA-DTA mouse model, with much earlier embryonic lethality. Therefore, loss of TFAP2C within the JZ affects proliferation and not apoptosis of trophoblasts derived from TPBPA^{+} progenitors. The fact that there is no apoptosis in the JZ and the remnant cells are no longer TPBPA^{+} suggests that loss of TFAP2C directly leads to a loss of *Tpbpa* expression.

Loss of TFAP2C results in a severe deficit of hormones. These are synthesized by the TGCs and SpT cells in the mouse placenta and syncytiotrophoblast cells in the human placenta (Kromer et al., 1996; Wynne et al., 2006; Zhou et al., 1997). In humans, reduced levels of placental lactogens and pregnancy-specific glycoproteins in the maternal blood are associated with impaired placental function, leading to conditions such as IUGR and pre-eclampsia (Bersinger and Odegard, 2004; Pihl et al., 2009). Upon loss of TFAP2C, we see reduced number of SpA-TGCs, suggesting inefficient vascular remodeling, leading to restricted blood flow into the placenta. The increased expression of *Vegfa* and *Pdgfa* transcripts upon loss of TFAP2C are most likely a compensation for the inefficient angiogenesis and vascular remodeling.

Expression of imprinted genes has been shown to be crucial in the development of placenta. *Ascl2*-null mutants die at E10.5 as a result of placental failure due to lack of an SpT layer, reduced labyrinth and an expansion of the P-TGC layer (Guillemot et al., 1994). Unlike the phenotype associated with a complete loss of *Ascl2*, we observed reduced levels of *Ascl2* upon loss of TFAP2C, which reduces the SpT and GCs in a similar manner but does not completely lack the JZ. Oh-McGinnis, also reported an expansion in P-TGC layer in *Ascl2*$^{-/-}$ placenta (Oh-McGinnis et al., 2011) which does not correlate with our finding where P-TGCs are unaffected. P-TGCs are also derived from TPBPA-negative population and hence could be compensated as the loss of TFAP2C is specifically in TPBPA^{+} cells in this model system. Interestingly, the placenta from *H19*$^{-/-}$ mice display increased number of GCs and glycogen reserves, which is correlated with an increase in AKT protein level (Esquiliano et al., 2009). Upon loss of TFAP2C, we observed an

Development (2016) 143, 787-798 doi:10.1242/dev.128553

increase in *H19* expression and a smaller placenta with reduced glycogen stores. We also found reduced expression of *Tex19.1* upon loss of TFAP2C. *Tex19.1* is a genome defense gene involved in placental development and embryos exhibit growth retardation with small placentae upon loss of *Tex19.1* because of a reduction in the number of SpT, GCs and S-TGCs (Reichmann et al., 2013). TFAP2C mutant placentae, however, do not show a reduction in S-TGCs. On the contrary, S-TGCs lining the maternal sinusoids seem to be increased in number in the TFAP2C mutant labyrinth. Deregulated levels of *SLC38A4*, a neutral amino acid transporter in the placenta, have been associated with abnormal fetal birth weight in humans (Desforges et al., 2006; Li et al., 2012).

Fig. 7 summarizes the role of TFAP2C in murine placental development. Although JZ has been shown to be essential for embryonic survival (Guillemot et al., 1994), its reduction by three quarters upon deletion of TFAP2C leads to growth retardation of the embryo. Here, we present a non-invasive genetic model of IUGR which allows the advantage of studying the growth-restricted embryos together with the control embryos within the same uterine setting, thus overcoming intraspecies heterogeneity and offering a more precise analysis. IUGR is often associated with an increased risk of metabolic disorders and cardiovascular diseases later in adulthood (Godfrey, 2002). Thus, our model representing IUGR is a useful tool in gaining further insights into fetal metabolic programming. Additionally, IUGR models such as this could allow us to answer key questions in the hypothesis of developmental origin of diseases.

MATERIALS AND METHODS

Animals

All experiments were conducted according to the German law of animal protection and in agreement with the approval of the local institutional animal care committees (Landesamt für Natur, Umwelt und Verbraucherschutz, North Rhine-Westphalia; approval ID: #8.87-50.10.31.08.238). The experiments were conducted in accordance with the International Guiding Principles for Biomedical Research Involving Animals as announced by the Society for the Study of Reproduction.

Genotyping and tissue preparation

129-SV *Tpbpa-Cre* transgenic mice (Simmons et al., 2007) and male B6 *K5-Cre* transgenic mouse (Ramirez et al., 2004) were crossed with female 129-SV *Tfap2c*$^{fl/fl}$ mice (Werling and Schorle, 2002) to generate *TpbpaCre:Tfap2c*$^{-/-}$ and *K5Cre:Tfap2c*$^{-/-}$ placentae, respectively, and the pregnant females were dissected at embryonic days E7.5-E18.5 (noon on the day of the vaginal plug was designated as E0.5). All animals used were 3-6 months old. Genotype of the embryos was determined by isolating tail DNA and performing PCR, using previously described primers listed in Table S5 (Werling and Schorle, 2002). Tissue preparation and histology staining was done using standard protocols as described in supplementary Materials and Methods.

PAS reaction and glycogen extraction

For the detection of glycogen stores in the cells of the placentae, routine PAS (periodic acid-Schiff) reaction was performed (Autostainer 480, Medac, Germany). Briefly, the sections were deparaffinized, rehydrated with several ethanol steps, incubated in periodic acid, washed in tap water, incubated in Schiff reagent and counterstained with hematoxylin. The glycogen was

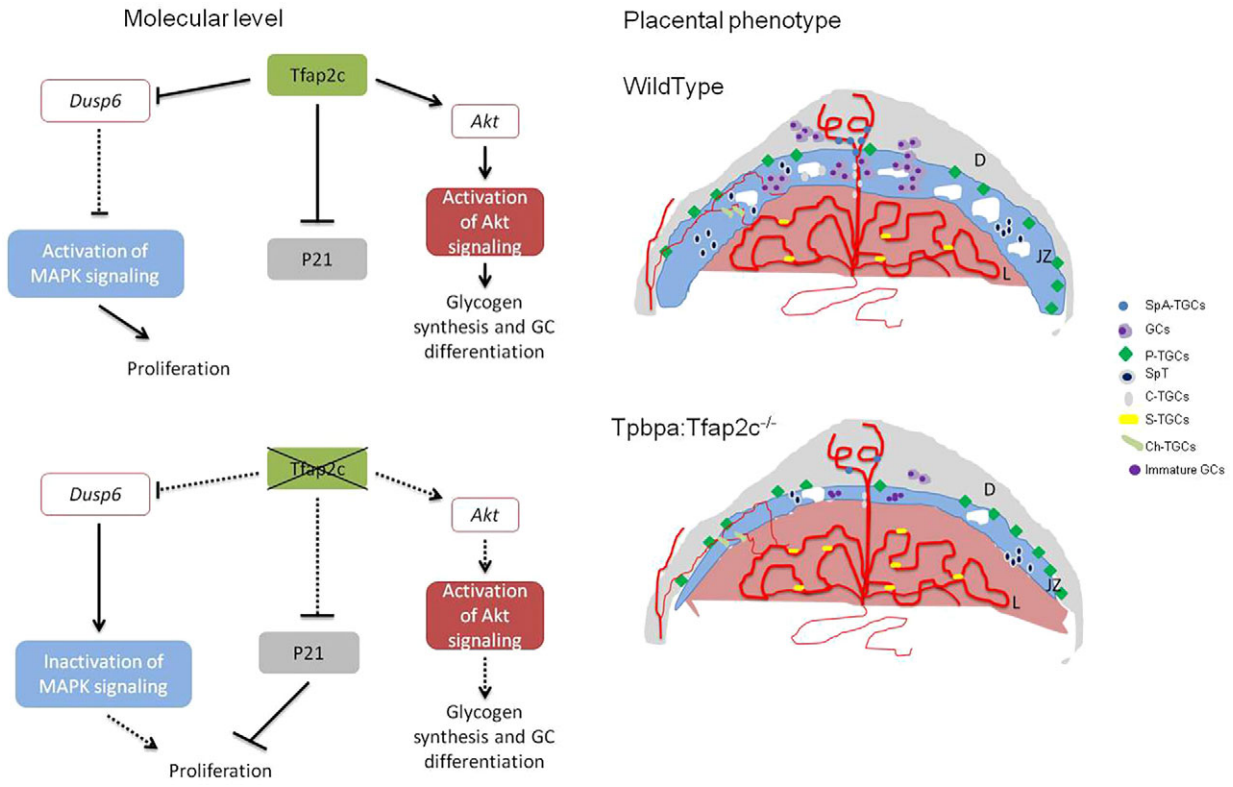

Fig. 7. Functional role of TFAP2C in mouse placenta. TFAP2C controls cell proliferation by repressing *Cdkn1a* and negative regulators of the MAPK pathway including *Dusp6*. TFAP2C also controls differentiation, especially of the GCs, by promoting AKT signaling involved in synthesis of glycogen stores. Thus, loss of TFAP2C in the murine JZ progenitor TPBPA^{+} cells reduces the proliferation of trophoblasts, including SpT, SpA-TGCs, C-TGCs and GCs, but not P-TGCs, as they are additionally derived from the TPBPA^{-} cell population. The Ch-TGCs are unaffected and the number of S-TGCs in the labyrinth is slightly increased. The GCs are not able to synthesize sufficient glycogen stores. This results in placental insufficiency and the mutant embryos are born 19% lighter. D, decidua; JZ, junctional zone; L, labyrinth.

Development (2016) 143, 787-798 doi:10.1242/dev.128553

extracted from E14.5 whole placenta as previously described (Lo et al., 1970). Frozen placentae were dissolved into 30% KOH by boiling for 20-30 min. Samples were cooled and incubated on ice with 1.2 volumes of 95% ethanol for 30 min. The samples were centrifuged and the glycogen precipitate was dissolved in distilled water. The amount of glycogen was calculated using standard biochemical colorimetric assay with Phenol and sulphuric acid.

RNA *in situ* hybridization

Cryo sections of 10 µm thickness were cut from the frozen placentae and RNA *in situ* hybridization was performed according to the established protocol (Simmons et al., 2007). Detailed protocol described in supplementary Materials and Methods. The following probes were used: *Prl3d1* (Pl1), *Prl3b1* (Pl2), *Prl2c2* (Plf) and *Tpbpa* (Simmons et al., 2007).

TUNEL

The DeadEnd Colorimetric TUNEL system was used to detect apoptosis (Promega, G7130) according to the manufacturer's instructions.

Laser microdissection, RNA isolation and microarray analysis

Control and *Tpbpa:Tfap2c*$^{-/-}$ placentae from day E13.5 and E14.5 were collected, snap frozen in liquid nitrogen and stored at −80°C. Laser microdissection was performed as described previously (Kaiser et al., 2015). Detailed protocol is given in supplementary Materials and Methods. The samples of SpT and labyrinth area were collected separately and RNA extraction was performed immediately with the RNeasy Micro Kit (Qiagen). Additionally, whole placental RNA from E8.5 *K5Cre:Tfap2c*$^{-/-}$ mice was isolated using Trizol reagent method. 1 µl total RNA from laser microdissection *Tpbpa:Tfap2c*$^{-/-}$ sections and 1 µg RNA from E8.5 *K5Cre:Tfap2c*$^{-/-}$ placentae were used for cDNA synthesis by Revert Aid Premium (Fermentas, ThermoScientific). Maxima SYBR Green Master Mix (Fermentas, ThermoScientific) was used to perform quantitative real-time PCR (qRT-PCR) on ViiA 7 (Applied Biosystems, Life Technologies). For primer sequences, see Table S6. Expression of target genes was normalized to glyceraldehyde-3-phosphate dehydrogenase (GAPDH). Each reaction was performed in triplicate. Microarray analysis using Illumina Mouse WG-6 v2.0 expression bead chip was performed with 200 ng total RNA pooled from three different laser microdissected samples each of control and mutant placentae. Data pre-processing was performed using the lumi pipeline (Du et al., 2008) using quantile normalization and a variance stabilizing transformation (Lin et al., 2008). Scatter plots were generated using R v3.1.3 software (http://www.R-project.org). The package pheatmap available from CRAN was used to generate the heatmap. Log-transformed expression values were used for the preselected genes in the heatmap. Genes with fold change ≥1.5 $\log_2$ scale are represented in the heatmap. Microarray data generated in the course of this work were deposited in National Center for Biotechnology Information's Gene Expression Omnibus (GEO) database (Edgar et al., 2002) and are accessible through GEO Series accession number GSE70962.

Bisulfite sequencing

JZ from 8 serial sections of 20 µm each of control and *Tpbpa:Tfap2c*$^{-/-}$ placentae were scraped off and DNA was isolated using a QIAamp FFPE DNA isolation kit according to the manufacturer's protocol (Qiagen). 500 ng gDNA was used for bisulfite conversion using EZ DNA Methylation-Direct Kit (ZYMO Research) following the manufacturer's recommendations. Following conversion, bisulfite-converted DNA was PCR amplified (primer sequences in Table S6), cloned into pCR2.1 vector and sequenced. DNA methylation profile over 6 CpG islands in the *H19/Igf2* ICR region containing CTCF3 binding site was analyzed. Data analysis was performed using BISMA online tool (Rohde et al., 2008).

Chromatin immunoprecipitation (ChIP)

Trophoblast stem cells L5 were differentiated in standard medium for 5 days (Kubaczka et al., 2014). ChIP was performed by enzymatic shearing using ChIP kit (Cell Signaling, 9003S) according to the manufacturer's instructions. For immunoprecipitation (n=2), 5 µg antibody against TFAP2C (clone H77/sc-8977 X; Santa Cruz Biotechnology, Santa Cruz, USA) was used. As a negative control, a species-matched rabbit-IgG antibody provided with the kit was used (Cell Signaling, 9003S). Primers used for q-PCR following ChIP are listed in Table S6.

JAr cells and shRNA knockdown

Human choriocarcinoma JAr cells were provided by Dr Daniel Nettersheim and tested for contamination (Nettersheim et al., 2013) and were grown and maintained in DMEM medium (10% FCS, 1% penicillin/streptomycin, 200 mM L-glutamine) at 37°C and 5% CO_2. For knockdown of TFAP2C, two different shRNA constructs were used (Table S7). Production of VSV-G pseudotyped retroviral particles was as following: HEK293T cells (maintained in DMEM supplemented with 10% FCS, 2 mM L-glutamine, 1% penicillin/streptomycin) were seeded at 80-90% confluency and transfected after 6-7 h by calcium phosphate transfection with the following plasmids at a 9:9:1 ratio: (1) pRetroSuper, (2) pCMV gag-pol, (3) pCMV VSV-G. The medium was replenished the following day in the morning and afternoon. Viral supernatants were collected at day 2 after transfection and were filtered through a 0.45-µm syringe filter. Briefly, viral supernatants were added to the cells for 24 h followed by growth in normal medium. Selection was done using 1 µg/ml puromycin for 5 days after transduction and the proteins were harvested after 1 week of transduction. Western blotting was performed as previously described (Kuckenberg et al., 2010). Detailed protocol and antibodies are listed in supplementary Materials and Methods.

Statistical analysis

Statistical significance (P-value) was determined using the Student's t-test (unpaired two-tailed distribution for *Tpbpa:Tfap2c*$^{-/-}$ placentae and paired two-tailed distribution for *K5Cre:Tfap2c*$^{-/-}$ placentae). All data are represented as means±s.d. Values of $P \leq 0.05$ were considered to be statistically significant. All graphs were made using GraphPad Prism software.

Acknowledgements

We thank Gaby Beine and Susanne Steiner for excellent technical assistance and Angela Egert, Andrea Jaeger and Renate Gammel for helping with mouse work. Additionally, we thank Andrea Hoffmann, Department of Genomics, Life and Brain Center, Bonn for performing Illumina expression arrays.

Competing interests

The authors declare no competing or financial interests.

Author contributions

N.S. conducted the experiments, S.K. performed microarray dissection, S.S.M. generated scatter plot and heat maps, S.R. provided viral supernatants for knockdown, D.N. provided shRNA constructs, N.S., C.K., D.N., and H.S. designed the study. N.S., C.K., D.N., E.W. and H.S. interpreted the data and N.S. and H.S. wrote the manuscript.

Funding

This study was supported by the Deutsche Forschungsgemeinschaft (DFG) [Scho 503/12-1 and Wi 774/27-1].

Supplementary information

Supplementary information available online at
http://dev.biologists.org/lookup/suppl/doi:10.1242/dev.128553/-/DC1

References

Adamson, S. L., Lu, Y., Whiteley, K. J., Holmyard, D., Hemberger, M., Pfarrer, C. and Cross, J. C. (2002). Interactions between trophoblast cells and the maternal and fetal circulation in the mouse placenta. *Dev. Biol.* **250**, 358-373.

Aladjem, S. and Lueck, J. (1981). Morphologic characteristics of the normal term human trophoblast maintained in prolonged in vitro cultures. *Br. J. Obstet. Gynaecol.* **88**, 287-293.

Anson-Cartwright, L., Dawson, K., Holmyard, D., Fisher, S. J., Lazzarini, R. A. and Cross, J. C. (2000). The glial cells missing-1 protein is essential for branching morphogenesis in the chorioallantoic placenta. *Nat. Genet.* **25**, 311-314.

Arroyo, J. A. and Winn, V. D. (2008). Vasculogenesis and angiogenesis in the IUGR placenta. *Semin. Perinatol.* **32**, 172-177.

Auman, H. J., Nottoli, T., Lakiza, O., Winger, Q., Donaldson, S. and Williams, T. (2002). Transcription factor AP-2gamma is essential in the extra-embryonic lineages for early postimplantation development. *Development* **129**, 2733-2747.

Development (2016) 143, 787-798 doi:10.1242/dev.128553

Bersinger, N. A. and Odegard, R. A. (2004). Second- and third-trimester serum levels of placental proteins in preeclampsia and small-for-gestational age pregnancies. *Acta Obstet. Gynecol. Scand.* **83**, 37-45.

Biadasiewicz, K., Sonderegger, S., Haslinger, P., Haider, S., Saleh, L., Fiala, C., Pollheimer, J. and Knöfler, M. (2011). Transcription factor AP-2alpha promotes EGF-dependent invasion of human trophoblast. *Endocrinology* **152**, 1458-1469.

Cao, Z., Carey, T. S., Ganguly, A., Wilson, C. A., Paul, S. and Knott, J. G. (2015). Transcription factor AP-2gamma induces early Cdx2 expression and represses HIPPO signaling to specify the trophectoderm lineage. *Development* **142**, 1606-1615.

Carney, E. W., Prideaux, V., Lye, S. J. and Rossant, J. (1993). Progressive expression of trophoblast-specific genes during formation of mouse trophoblast giant cells in vitro. *Mol. Reprod. Dev.* **34**, 357-368.

Choi, I., Carey, T. S., Wilson, C. A. and Knott, J. G. (2012). Transcription factor AP-2gamma is a core regulator of tight junction biogenesis and cavity formation during mouse early embryogenesis. *Development* **139**, 4623-4632.

Coan, P. M., Conroy, N., Burton, G. J. and Ferguson-Smith, A. C. (2006). Origin and characteristics of glycogen cells in the developing murine placenta. *Dev. Dyn.* **235**, 3280-3294.

Crish, J., Conti, M. A., Sakai, T., Adelstein, R. S. and Egelhoff, T. T. (2013). Keratin 5-Cre-driven excision of nonmuscle myosin IIA in early embryo trophectoderm leads to placenta defects and embryonic lethality. *Dev. Biol.* **382**, 136-148.

Cross, D. A. E., Alessi, D. R., Cohen, P., Andjelkovich, M. and Hemmings, B. A. (1995). Inhibition of glycogen synthase kinase-3 by insulin mediated by protein kinase B. *Nature* **378**, 785-789.

Cross, J. C., Simmons, D. G. and Watson, E. D. (2003). Chorioallantoic morphogenesis and formation of the placental villous tree. *Ann. N. Y. Acad. Sci.* **995**, 84-93.

Daoud, G., Amyot, M., Rassart, E., Masse, A., Simoneau, L. and Lafond, J. (2005). ERK1/2 and p38 regulate trophoblasts differentiation in human term placenta. *J. Physiol.* **566**, 409-423.

Desforges, M., Lacey, H. A., Glazier, J. D., Greenwood, S. L., Mynett, K. J., Speake, P. F. and Sibley, C. P. (2006). SNAT4 isoform of system A amino acid transporter is expressed in human placenta. *Am. J. Physiol. Cell Physiol.* **290**, C305-C312.

Diehl, J. A., Cheng, M., Roussel, M. F. and Sherr, C. J. (1998). Glycogen synthase kinase-3beta regulates cyclin D1 proteolysis and subcellular localization. *Genes Dev.* **12**, 3499-3511.

Dong, Y., Zhang, L., Zhang, S., Bai, Y., Chen, H., Sun, X., Yong, W., Li, W., Colvin, S. C., Rhodes, S. J. et al. (2012). Phosphatase of regenerating liver 2 (PRL2) is essential for placental development by down-regulating PTEN (Phosphatase and Tensin Homologue Deleted on Chromosome 10) and activating Akt protein. *J. Biol. Chem.* **287**, 32172-32179.

Du, P., Kibbe, W. A. and Lin, S. M. (2008). lumi: a pipeline for processing Illumina microarray. *Bioinformatics* **24**, 1547-1548.

Eckert, D., Buhl, S., Weber, S., Jäger, R. and Schorle, H. (2005). The AP-2 family of transcription factors. *Genome Biol.* **6**, 246.

Edgar, R., Domrachev, M. and Lash, A. E. (2002). Gene Expression Omnibus: NCBI gene expression and hybridization array data repository. *Nucleic Acids Res.* **30**, 207-210.

Esquiliano, D. R., Guo, W., Liang, L., Dikkes, P. and Lopez, M. F. (2009). Placental glycogen stores are increased in mice with H19 null mutations but not in those with insulin or IGF type 1 receptor mutations. *Placenta* **30**, 693-699.

Gabory, A., Ripoche, M.-A., Le Digarcher, A., Watrin, F., Ziyyat, A., Forne, T., Jammes, H., Ainscough, J. F. X., Surani, M. A., Journot, L. et al. (2009). H19 acts as a trans regulator of the imprinted gene network controlling growth in mice. *Development* **136**, 3413-3421.

Gasperowicz, M., Surmann-Schmitt, C., Hamada, Y., Otto, F. and Cross, J. C. (2013). The transcriptional co-repressor TLE3 regulates development of trophoblast giant cells lining maternal blood spaces in the mouse placenta. *Dev. Biol.* **382**, 1-14.

Godfrey, K. M. (2002). The role of the placenta in fetal programming-a review. *Placenta* **23** Suppl. A, S20-S27.

Guillemot, F., Nagy, A., Auerbach, A., Rossant, J. and Joyner, A. L. (1994). Essential role of Mash-2 in extraembryonic development. *Nature* **371**, 333-336.

Hemberger, M., Hughes, M. and Cross, J. C. (2004). Trophoblast stem cells differentiate in vitro into invasive trophoblast giant cells. *Dev. Biol.* **271**, 362-371.

Hu, D. and Cross, J. C. (2011). Ablation of Tpbpa-positive trophoblast precursors leads to defects in maternal spiral artery remodeling in the mouse placenta. *Dev. Biol.* **358**, 231-239.

Kaiser, S., Koch, Y., Kühnel, E., Sharma, N., Gellhaus, A., Kuckenberg, P., Schorle, H. and Winterhager, E. (2015). Reduced gene dosage of Tfap2c impairs trophoblast lineage differentiation and alters maternal blood spaces in the mouse placenta. *Biol. Reprod.* **93**, 31.

Keyse, S. M. (2008). Dual-specificity MAP kinase phosphatases (MKPs) and cancer. *Cancer Metastasis Rev.* **27**, 253-261.

Kidder, B. L. and Palmer, S. (2010). Examination of transcriptional networks reveals an important role for TCFAP2C, SMARCA4, and EOMES in trophoblast stem cell maintenance. *Genome Res.* **20**, 458-472.

Kingdom, J., Huppertz, B., Seaward, G. and Kaufmann, P. (2000). Development of the placental villous tree and its consequences for fetal growth. *Eur. J. Obstet. Gynecol. Reprod. Biol.* **92**, 35-43.

Kita, N., Mitsushita, J., Ohira, S., Takagi, Y., Ashida, T., Kanai, M., Nikaido, T. and Konishi, I. (2003). Expression and activation of MAP kinases, ERK1/2, in the human villous trophoblasts. *Placenta* **24**, 164-172.

Kotani, T., Iwase, A., Ino, K., Sumigama, S., Yamamoto, E., Hayakawa, H., Nagasaka, T., Itakura, A., Nomura, S. and Kikkawa, F. (2009). Activator protein-2 impairs the invasion of a human extravillous trophoblast cell line. *Endocrinology* **150**, 4376-4385.

Kromer, B., Finkenzeller, D., Wessels, J., Dveksler, G., Thompson, J. and Zimmermann, W. (1996). Coordinate expression of splice variants of the murine pregnancy-specific glycoprotein (PSG) gene family during placental development. *Eur. J. Biochem.* **242**, 280-287.

Kubaczka, C., Senner, C., Araúzo-Bravo, M. J., Sharma, N., Kuckenberg, P., Becker, A., Zimmer, A., Brüstle, O., Peitz, M., Hemberger, M. et al. (2014). Derivation and maintenance of murine trophoblast stem cells under defined conditions. *Stem Cell Rep.* **2**, 232-242.

Kuckenberg, P., Buhl, S., Woynecki, T., van Furden, B., Tolkunova, E., Seiffe, F., Moser, M., Tomilin, A., Winterhager, E. and Schorle, H. (2010). The transcription factor TCFAP2C/AP-2gamma cooperates with CDX2 to maintain trophectoderm formation. *Mol. Cell. Biol.* **30**, 3310-3320.

Kuckenberg, P., Kubaczka, C. and Schorle, H. (2012). The role of transcription factor Tcfap2c/TFAP2C in trophectoderm development. *Reprod. Biomed. Online* **25**, 12-20.

Lescisin, K. R., Varmuza, S. and Rossant, J. (1988). Isolation and characterization of a novel trophoblast-specific cDNA in the mouse. *Genes Dev.* **2**, 1639-1646.

Li, Z., Lai, G., Deng, L., Han, Y., Zheng, D. and Song, W. (2012). Association of SLC38A4 and system A with abnormal fetal birth weight. *Exp. Ther. Med.* **3**, 309-313.

Lin, S. M., Du, P., Huber, W. and Kibbe, W. A. (2008). Model-based variance-stabilizing transformation for Illumina microarray data. *Nucleic Acids Res.* **36**, e11.

Lo, S., Russell, J. C. and Taylor, A. W. (1970). Determination of glycogen in small tissue samples. *J. Appl. Physiol.* **28**, 234-236.

Mayhew, T. M., Charnock-Jones, D. S. and Kaufmann, P. (2004). Aspects of human fetoplacental vasculogenesis and angiogenesis. III. Changes in complicated pregnancies. *Placenta* **25**, 127-139.

Nettersheim, D., Heukamp, L. C., Fronhoffs, F., Grewe, M. J., Haas, N., Waha, A., Honecker, F., Waha, A., Kristiansen, G. and Schorle, H. (2013). Analysis of TET expression/activity and 5mC oxidation during normal and malignant germ cell development. *PLoS ONE* **8**, e82881.

Oh-McGinnis, R., Bogutz, A. B. and Lefebvre, L. (2011). Partial loss of Ascl2 function affects all three layers of the mature placenta and causes intrauterine growth restriction. *Dev. Biol.* **351**, 277-286.

Pattillo, R. A., Gey, G. O., Delfs, E., Huang, W. Y., Hause, L., Garancis, J., Knoth, M., Amatruda, J., Bertino, J., Friesen, H. G. et al. (1971). The hormone-synthesizing trophoblastic cell in vitro: a model for cancer research and placental hormone synthesis. *Ann. N. Y. Acad. Sci.* **172**, 288-298.

Phillips, J. E. and Corces, V. G. (2009). CTCF: master weaver of the genome. *Cell* **137**, 1194-1211.

Pihl, K., Larsen, T., Laursen, I., Krebs, L. and Christiansen, M. (2009). First trimester maternal serum pregnancy-specific beta-1-glycoprotein (SP1) as a marker of adverse pregnancy outcome. *Prenat. Diagn.* **29**, 1256-1261.

Ramirez, A., Page, A., Gandarillas, A., Zanet, J., Pibre, S., Vidal, M., Tusell, L., Genesca, A., Whitaker, D. A., Melton, D. W. et al. (2004). A keratin K5Cre transgenic line appropriate for tissue-specific or generalized Cre-mediated recombination. *Genesis* **39**, 52-57.

Reichmann, J., Reddington, J. P., Best, D., Read, D., Ollinger, R., Meehan, R. R. and Adams, I. R. (2013). The genome-defence gene Tex19.1 suppresses LINE-1 retrotransposons in the placenta and prevents intra-uterine growth retardation in mice. *Hum. Mol. Genet.* **22**, 1791-1806.

Rohde, C., Zhang, Y., Jurkowski, T. P., Stamerjohanns, H., Reinhardt, R. and Jeltsch, A. (2008). Bisulfite sequencing Data Presentation and Compilation (BDPC) web server–a useful tool for DNA methylation analysis. *Nucleic Acids Res.* **36**, e34.

Rossant, J. and Cross, J. C. (2001). Placental development: lessons from mouse mutants. *Nat. Rev. Genet.* **2**, 538-548.

Saba-El-Leil, M. K., Vella, F. D. J., Vernay, B., Voisin, L., Chen, L., Labrecque, N., Ang, S.-L. and Meloche, S. (2003). An essential function of the mitogen-activated protein kinase Erk2 in mouse trophoblast development. *EMBO Rep.* **4**, 964-968.

Schemmer, J., Arauzo-Bravo, M. J., Haas, N., Schafer, S., Weber, S. N., Becker, A., Eckert, D., Zimmer, A., Nettersheim, D. and Schorle, H. (2013). Transcription factor TFAP2C regulates major programs required for murine fetal germ cell maintenance and haploinsufficiency predisposes to teratomas in male mice. *PLoS One* **8**, e71113.

Development (2016) 143, 787-798 doi:10.1242/dev.128553

Simmons, D. G., Fortier, A. L. and Cross, J. C. (2007). Diverse subtypes and developmental origins of trophoblast giant cells in the mouse placenta. *Dev. Biol.* **304**, 567-578.

Spanheimer, P. M., Cyr, A. R., Gillum, M. P., Woodfield, G. W., Askeland, R. W. and Weigel, R. J. (2014). Distinct pathways regulated by RET and estrogen receptor in luminal breast cancer demonstrate the biological basis for combination therapy. *Ann. Surg.* **259**, 793-799.

Takahashi, K., Kobayashi, T. and Kanayama, N. (2000). p57(Kip2) regulates the proper development of labyrinthine and spongiotrophoblasts. *Mol. Hum. Reprod.* **6**, 1019-1025.

Tanaka, M., Gertsenstein, M., Rossant, J. and Nagy, A. (1997). Mash2 acts cell autonomously in mouse spongiotrophoblast development. *Dev. Biol.* **190**, 55-65.

Werling, U. and Schorle, H. (2002). Transcription factor gene AP-2 gamma essential for early murine development. *Mol. Cell. Biol.* **22**, 3149-3156.

White, T. E., Saltzman, R. A., Di Sant'Agnese, P. A., Keng, P. C., Sutherland, R. M. and Miller, R. K. (1988). Human choriocarcinoma (JAr) cells grown as multicellular spheroids. *Placenta* **9**, 583-598.

Wynne, F., Ball, M., McLellan, A. S., Dockery, P., Zimmermann, W. and Moore, T. (2006). Mouse pregnancy-specific glycoproteins: tissue-specific expression and evidence of association with maternal vasculature. *Reproduction* **131**, 721-732.

Yang, Z.-Z., Tschopp, O., Hemmings-Mieszczak, M., Feng, J., Brodbeck, D., Perentes, E. and Hemmings, B. A. (2003). Protein kinase B alpha/Akt1 regulates placental development and fetal growth. *J. Biol. Chem.* **278**, 32124-32131.

Zhou, G.-Q., Baranov, V., Zimmermann, W., Grunert, F., Erhard, B., Mincheva-Nilsson, L., Hammarstrom, S. and Thompson, J. (1997). Highly specific monoclonal antibody demonstrates that pregnancy-specific glycoprotein (PSG) is limited to syncytiotrophoblast in human early and term placenta. *Placenta* **18**, 491-501.

Supplementary Experimental procedure

Tissue preparation, Histology and Immunohistochemistry

Embryos and placentae were harvested in ice cold 1x Phosphate buffered saline (PBS) from timed mating and fixed in 4% paraformaldehyde/PBS overnight at 4°C. Tissues were washed with PBS thrice and cut into two halves for paraffin and cryo embedding. For paraffin embedding, tissues were dehydrated through a graded ethanol series and embedded as paraffin blocks. 4 µm sections were cut and processed for histology and IHC. For cryo sections, tissues were incubated overnight at 4°C in 10% and 25% sucrose respectively followed by freezing in OCT in dry ice. Blocks were stored at -80°C and 10 µm sections were cut on Superfrost slides for in situ hybridization (ISH). Histological sections were stained with Hematoxylin and Eosin (H/E) using standard protocol. IHC was performed as published previously (Kuckenberg et al., 2010). 4 µm hydrated deparaffinized paraffin sections following antigen retrieval were incubated with primary antibody against Tfap2c (1:250; sc53162-6E4/4, Santa Cruz), Ki-67(1:250; TEC-3, DAKO, Germany), CD-31(1:20; SZ31, Dianova, Germany), pERK1/2(1:50, #4370 cell signaling), and pAKT(1:50,# 4060, cell signaling) overnight at 4 °C. Anti-rabbit (1:500; DAKO, Hamburg, Germany) and anti-rat (1:200; DAKO) secondary antibodies were used for 30 minutes at room temperature. Signals were visualized using a Vectastain ABC kit (Vector Laboratories, Germany). Sections were photographed using Diskus software (Hilden, Germany).

ISH

Briefly, sections were rehydrated in 1x PBS, fixed in 4% PFA and incubated with 30µg/ml Proteinase K for 10 minutes at 37°C. Each step was followed by careful washing with PBS for 5 minutes each. Sections were hybridized overnight with DIG labeled probes (2ng/µl) at 65°C. Following day, sections were washed, incubated with RNaseA and subsequently blocked for an hour at room temperature, incubated with anti-DIG antibody conjugated to alkaline phosphatase (1:2000; Roche, Mannheim, Germany) at 4°C overnight. Sections were washed, developed and counter stained with NuclearFastRed (Sigma, Germany) and mounted with Entellan (Merck, Germany).

TUNEL

Cryo sections were fixed in 4%PFA for 15 minutes and incubated with 20 µg/ml of proteinase K for 15 minutes and washed with PBS. For positive control, sections were treated with DNAse 1 for 15 minutes and rinsed with PBS The sections were incubated with equilibration buffer for 5–10 minutes following incubation with rTdT (Terminal Deoxynucleotidyl Transferase, Recombinant) reaction mix including rTdT enzyme and biotinylated nucleotide mix in a humidified atmosphere at 37 °C for 1 hour. The sections were further washed with 2× SSC for 15 minutes at room temperature. The endogenous peroxidase activity was blocked with 0.3% hydrogenperoxide followed by subsequent washing step in PBS thrice for 5 minutes each. The sections were then incubated with Streptavidin HRP for 30 minutes and staining was done with diaminobenzidine followed by washing and mounting the sections.

Laser microdissection

10 µm sections were cut with a cryomicrotome (Leica CM 1850 UV, Germany) and collected on membrane coated glass slides (Membrane Slides 1.0 PEN, Zeiss, Germany). The samples were fixed at -20° C with Ethanol and stained with Cresyl violet (Merck, Germany) according to the manufacturer's instructions. For preservation and improving the visualization of the tissue under the microscope, the sections were mounted with Liquid Cover Glass (Zeiss, Germany). Laser Microdissection was performed with the PALM MicroBeam System (Zeiss, Germany) with an Axiovert microscope (Zeiss, Germany). The software used was PALM RoboSoftware 4.2 (Zeiss, Germany).

Western Blot

For protein analysis, 25 µg of protein was run on a 10% SDS-PAGE and transferred onto a nitrocellulose membrane. Primary antibodies were used to detect TFAP2C (1:500, 6E4/4 sc-53162, Santa Cruz), pERK1/2 (1:1000, #4370, cell signaling), ERK1/2 (1:1000, #9102, cell signaling), pP38 (1:1000, #9211, cell signaling,, P38 (1:1000, #9212, cell signaling), pAKT (1:1000, #4060, cell signaling), AKT (1:1000, #4691, cell signaling) and B-ACTIN (1:50000; AC-15, Sigma Aldrich).

HRP conjugated secondary antibodies were used (anti-mouse 1:1000; anti rabbit 1:2000, DAKO) and the membrane was incubated with Pierce- Super Signal West Pico chemiluminescent substrate (Thermo scientific) and the signal was detected using ChemiDoc MP imaging system (BIO-RAD).

Softwares:

Web based GeneMANIA (Warde-Farley et al., 2010) (www.genemania.org), String (Jensen et al., 2009) (www.string-db.org) and rVista algorithm (Loots and Ovcharenko, 2004) softwares were used.

Supplementary figures

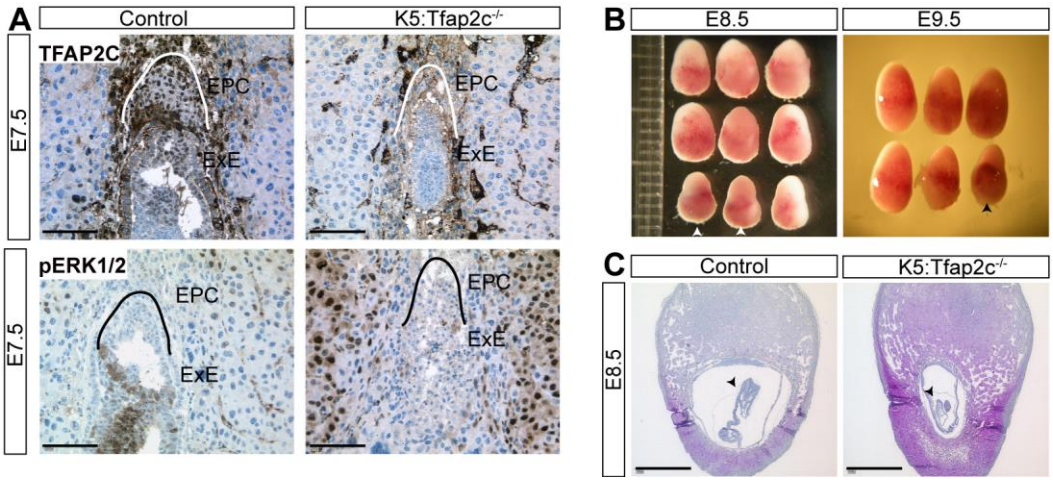

Fig. S1: Smaller implantation in K5Cre:Tfap2c$^{-/-}$ placentae. (A) IHC against TFAP2C and pERK1/2 at E7.5 placental sections of K5Cre:Tfap2c$^{-/-}$ and control. Scale bar- 100µm (B) Whole implantation isolated from K5Cre:Tfap2c$^{-/-}$ E8.5 and E9.5 respectively. Arrowheads show smaller K5Cre:Tfap2c$^{-/-}$ implantation. (C) H/E stained placentae of control and K5Cre:Tfap2c$^{-/-}$ at E8.5. Arrowheads indicate smaller embryo in K5Cre:Tfap2c$^{-/-}$. Scale bar 1000µm.

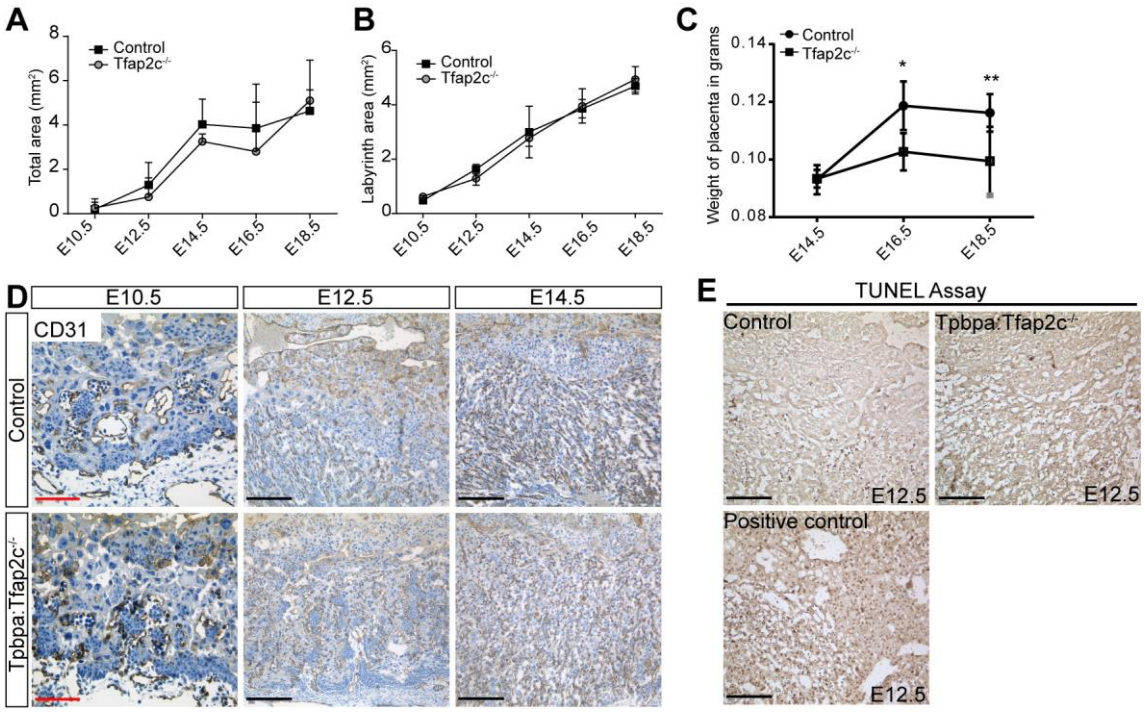

Fig. S2: Analysis of Tpbpa:Tfap2c$^{-/-}$ placentae. (A) Total area of the control and Tpbpa:Tfap2c$^{-/-}$ placentae at E10.5 (n=2 each), E12.5 (n=3 each), E14.5 (n=6 each), E16.5 (n=4 each) and E18.5 (n=6 each). (B) Labyrinth area of the control and Tpbpa:Tfap2c$^{-/-}$ placentae at E10.5 (n=2 each), E12.5 (n=3 each), E14.5 (n=6 each), E16.5 (n=4 each) and E18.5 (n=6 each). (C) Weight of Tpbpa:Tfap2c$^{-/-}$ and control placentae show lighter Tpbpa:Tfap2c$^{-/-}$ placenta at E16.5 (n=11 control, n=3 mutant) and E18.5 (n=13 control, n=7 mutant). (D) IHC against CD-31 on paraffin embedded sections at E10.5, E12.5 and E14.5 respectively in control and Tpbpa:Tfap2c$^{-/-}$ placentae. (E) TUNEL staining to detect apoptotic cells on cryo embedded E12.5 control and Tpbpa:Tfap2c$^{-/-}$ placentae with positive control. Black scale bar- 200 µm, Red scale bar- 100 µm. Data are represented as mean +/- SD. ** $p \leq 0.005$,* $p \leq 0.05$

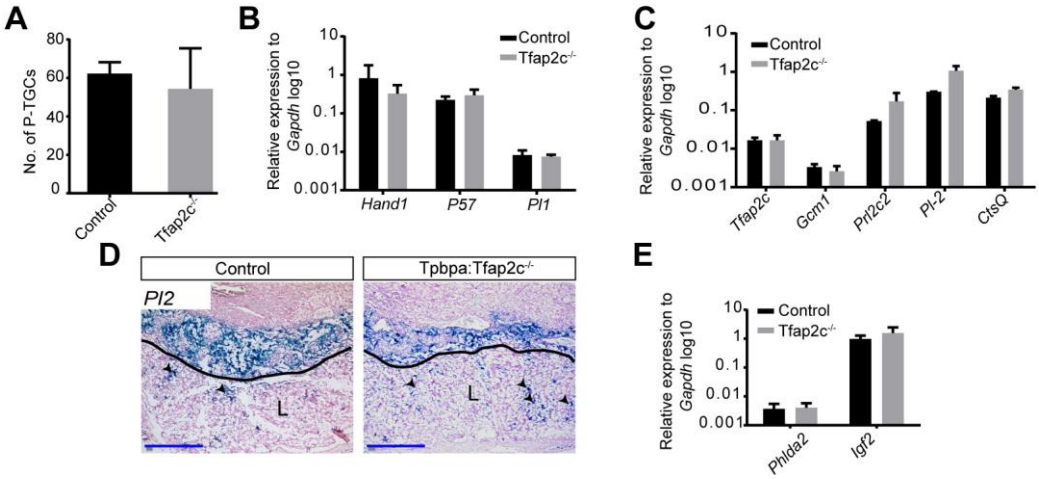

Fig. S3: Analysis of JZ and labyrinth of Tpbpa:Tfap2c$^{-/-}$ placentae. (A) Quantification of P-TGCs on E12.5 Tpbpa:Tfap2c$^{-/-}$ and control placentae by counting the number of P-TGCs on 3 different sections each. (B) Samples were obtained by laser microdissection of SpT from E14.5 Tpbpa:Tfap2c$^{-/-}$ and control placentae (n=4 each) and expression levels relative to *Gapdh* in log10 scale were measured. *Hand1*, *p57 and Pl1* did not show any deregulation compared to the control placentae. (C) Samples were obtained by laser microdissection of Labyrinth from E14.5 Tpbpa:Tfap2c$^{-/-}$ and control placentae (n=2 Tpbpa:Tfap2c$^{-/-}$ and n=3 control) and expression levels (relative to *Gapdh*, log10 scale) of *Tfap2c, Gcm1, Prl2c2, Pl2* and *CtsQ* were measured. Increased expression of *Prl2c2* and *Pl2* is detected. (D) In situ hybridization on cryo embedded sections at E14.5 against *Pl2*. Arrows show increased number of *Pl2* positive cells in the labyrinth of Tpbpa:Tfap2c$^{-/-}$ placentae compared to the control. (E) Samples were obtained by laser microdissection of JZ from E14.5 Tpbpa:Tfap2c$^{-/-}$ and control placentae (n=3 each) and expression levels (relative to *Gapdh*, log10 scale) of *Phlda2* and *Igf2* were measured. L- labyrinth, Blue scale bar- 500 µm. Data are represented as mean +/- SD.

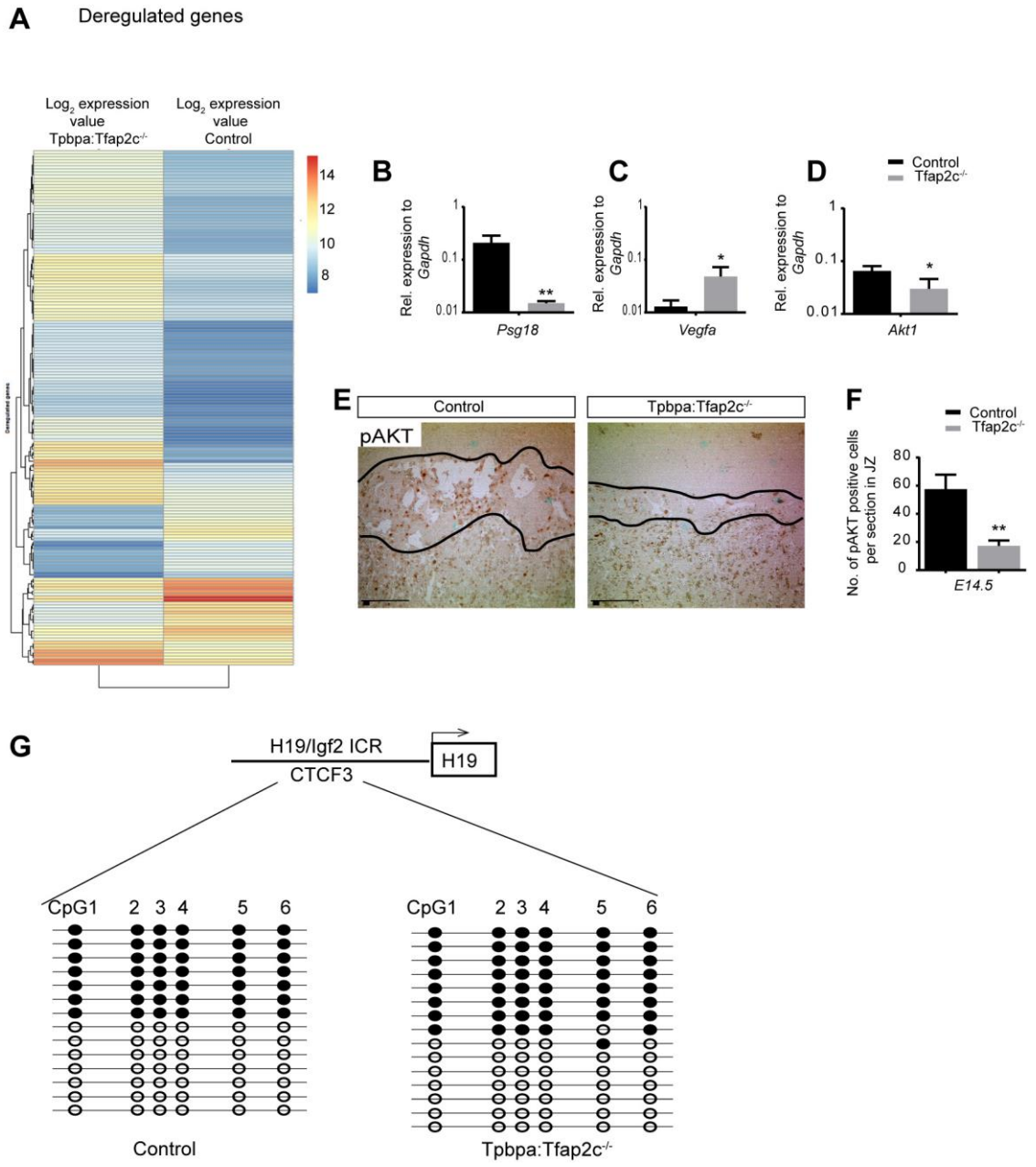

Fig. S4: Validation of genes deregulated in the microarray analysis of laser microdissected JZ from control and Tpbpa:Tfap2c$^{-/-}$ placentae at E14.5. (A) Heat map showing expression values of all deregulated genes in Log_2 scale in control and Tpbpa:Tfap2c$^{-/-}$ placentae. Log-transformed expression values are presented on a scale of 8 to 14. Upregulated genes are indicated in shades of red; downregulated in blue. (B) Samples were obtained by laser microdissection of SpT from E14.5 Tpbpa:Tfap2c$^{-/-}$ and control placentae (n=4 each) and expression levels relative to *Gapdh* were measured by qRT-PCR. Note significant downregulation of *Psg18*, (C) *Vegfa* and (D) *Akt1*. (E) IHC against pAKT on placental sections E14.5. (F) Quantification of pAKT positive cells.Three different high magnification areas were counted each. Data are represented as mean +/- SD. ** $p \leq 0.005$,* $p \leq 0.05$. (G) Graphical representation of % methylation of CTCF3 region in H19 ICR domain in JZ of Tpbpa:Tfap2c$^{-/-}$ (n=15) and control placentae (n=16).

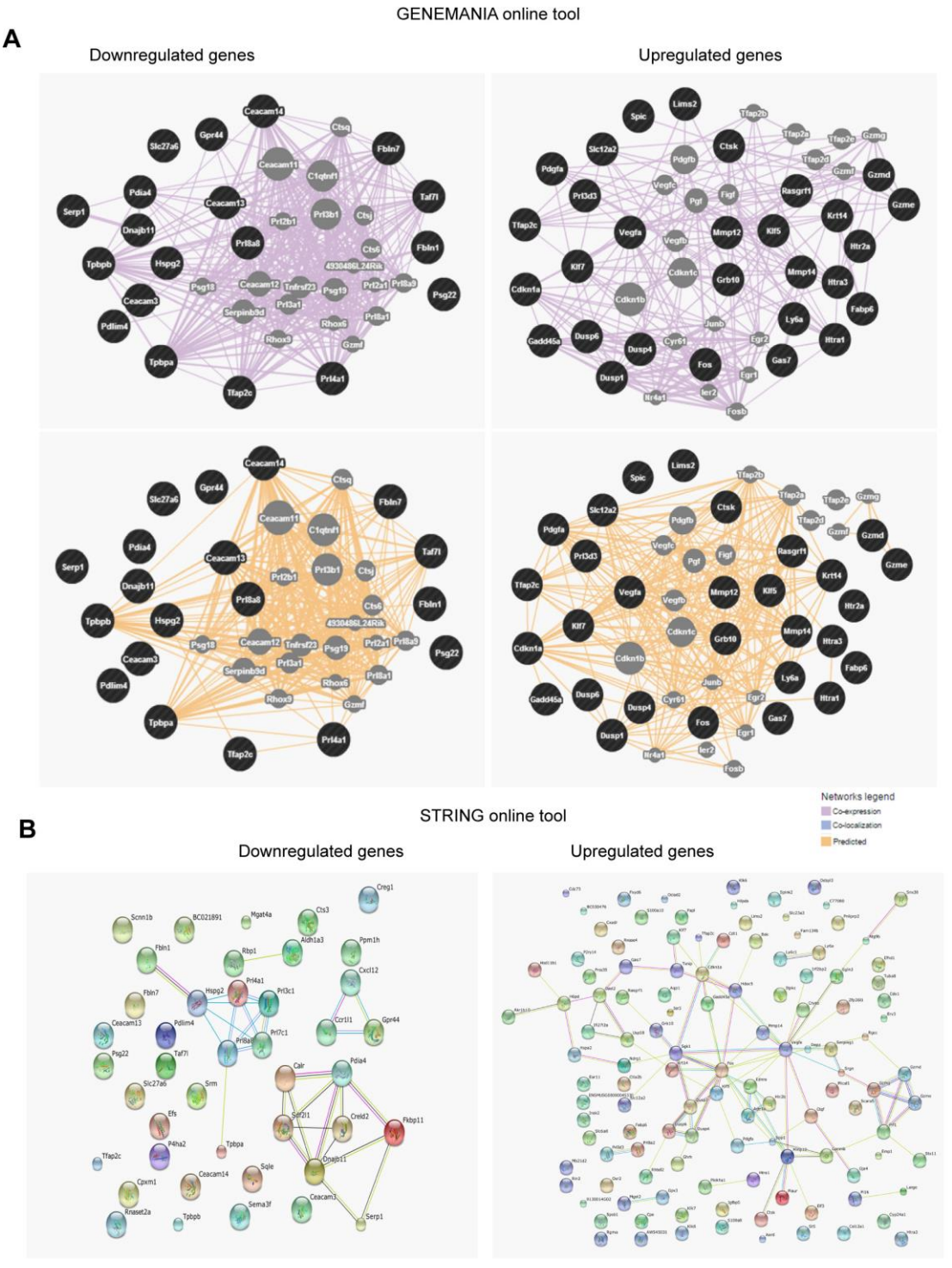

Fig. S5: Interactive analysis of deregulated genes from expression microarray data. (A) Interactive gene network analysis of up and downregulated genes using GENEMANIA online tool. Note linked co-expression of Tfap2c and Tpbpa in downregulated genes. Purple lines indicate co-expression and orange lines indicate predicted interaction among the genes. (B) Interactive known and predicted protein- protein association using STRING online tool.

Table S1: List of upregulated genes in the JZ of mutant placentae at E13.5
Table S2: List of downregulated genes in the JZ of mutant placentae at E13.5
Table S3: GO grouping of differentially regulated genes identified in murine placental JZ microarray analysis
Table S4: Deregulated genes with fold change and p value in qRT-PCR relative to the control
Table S5: Sequence of genotyping primers
Table S6: Gene name and sequences of primers used for quantitative RT- PCR and ChIP and Bisulfite sequencing
Table S7: shRNA oligonucleotide sequence

Table S1: List of genes upregulated in the JZ of mutant placentae

Gene symbol	FC>1.5 (Log2
Osbpl3	**1.509086**
C77080	1.523591
H6pd	1.526885
Prl3d3	1.528163
Snx30	1.531885
Slc6a8	1.537295
Grb10	1.542198
Slc12a2	1.554466
Sgk1	1.565943
Plaur	1.567605
Rhbdl2	1.575135
Mmp14	1.575289
Ly6c1	1.578245
4933402E13Rik	1.578724
LOC385615	1.58095
Rasgrf1	1.588314
Atg9b	1.589724
Gzmd	1.594451
Cdt1	1.595864
4732462B05Rik	1.596131
Ndrg1	1.599179
Rnase4	1.602184
Hspa2	1.60634
Cdo1	1.607689
Plekha1	1.608894
Oasl2	1.612556
Irak2	1.615824
Cxadr	1.624538
Prf1	1.657681
2310005E10Rik	1.657707
Gadd45a	1.670023
Irf2bp2	1.676604

Irak2	1.67875
Aqp1	1.705648
Cdc73	1.706444
Egln3	1.707686
Elf3	1.711483
Tuba8	1.721988
Htr2b	1.725925
Cyp24a1	1.72717
Usp18	1.72859
2310016C08Rik	1.734629
Large	1.740121
Prl3d3	1.740349
Cdkn1a	1.741578
Spsb1	1.743703
Ociad2	1.746128
St5	1.747912
Itpkc	1.751357
1600021P15Rik	1.773339
Ndrl	1.775981
Klf5	1.782944
Klf7	1.783327
Gzme	1.784651
Mical1	1.785555
1600014E20Rik	1.789272
Fxyd6	1.790198
BC030476	1.790865
Serping1	1.798993
Srgn	1.807363
Gzmd	1.825638
St5	1.839717
B230343A10Rik	1.84686
Dusp4	1.84861
Dusp6	1.860065
Rasgrf1	1.870452
Gpnmb	1.87048
Ctgf	1.873728
Aard	1.893147
Bok	1.898854
Spp1	1.904676
Klk7	1.9048
Osr2	1.905259
Stx11	1.914442
Klf7	1.915583
Zfp36l1	1.918171
Prss35	1.924599
S100a10	1.931051

Ghrh	1.937728
Hsd11b1	1.938285
Hsd11b1	1.95428
P2ry14	1.955215
Cpe	1.96212
C330005M16Rik	1.968196
Osbpl3	1.969108
Cryab	1.970954
Txnip	1.975591
Hdac5	1.986672
Ly6a	1.991316
Slc23a3	1.998663
S100a8	2.016638
Hsd11b1	2.021868
Gas7	2.026153
Fabp6	2.048584
Lims2	2.066802
Klf7	2.068018
Txnip	2.088046
Ier3	2.090304
Pi16	2.099015
Ear11	2.104489
Ctgf	2.116343
Dusp1	2.116575
Htra1	2.117235
Vegfa	2.124982
Klk6	2.130946
Scara5	2.135991
Mgst2	2.147432
Ctsk	2.156731
Mmp12	2.160021
Rgma	2.161246
Efhd1	2.180658
Prl3d3	2.183273
Pdgfa	2.187754
Gpx3	2.191067
Rin2	2.23222
4930486L24Rik	2.254293
Htra3	2.256029
Gzmg	2.275722
Pnliprp2	2.285754
Prl8a2	2.363383
Htra1	2.425347
scl0001849.1_2273	2.436885
Dusp4	2.460281
Krt14	2.473251

Lims2	2.612874
8430408G22Rik	2.622677
Gas7	2.630254
Igfbp5	2.639024
Prss18	2.656949
Agtr1a	2.661501
Lims2	2.697922
Ednra	2.761526
4930539E08Rik	3.055416
Gja4	3.132141
Col12a1	3.140382
Fos	3.192744
Ctla2b	3.2266
Pnliprp2	3.275906
Igfbp5	3.32744
1190002H23Rik	3.392156
Igfbp5	3.461613
Fam134b	3.552477
Ifi27	4.147568
Emp1	4.181227
Klk8	4.650642
Spink2	5.626195

Table S2: List of genes downregulated in the JZ of mutant placentae

Gene symbol	FC>1.5 (Log2)
eGFP	**-3.77727**
Cts3	-3.7038
LOC381852	-3.06463
Prlpc3	-2.88441
Creg1	-2.73667
Ceacam13	-2.68573
Fkbp11	-2.58183
Ceacam14	-2.52696
Ceacam13	-2.41975
Creld2	-2.37883
Calr	-2.35118
Sdf2l1	-2.32642
BC021891	-2.28505
Sema3f	-2.27968
Ceacam3	-2.23943
Fbln7	-2.22116
Creld2	-2.20439
P4ha2	-2.18194
Scnn1b	-2.17906
Cxcl12	-2.17149
Prl4a1	-2.16109
C030002B11Rik	-2.13341
Sema3f	-2.10653
Psg22	-2.08036
Pdia4	-2.02606
Ceacam14	-2.00069
Prl3c1	-1.97935
Aldh1a3	-1.94388
Prl7c1	-1.94014
P4ha2	-1.92095
Tpbpb	-1.90947
Dnajb11	-1.86672
Pdlim4	-1.85605
Efs	-1.84588
Ccr1l1	-1.80664
9530018I07Rik	-1.7933
Rbp1	-1.67397
Fbln1	-1.66694
Tpbpa	-1.653
Fbln1	-1.63775
Hspg2	-1.63722
Gpr44	-1.61621
Slc27a6	-1.59768

LOC100044439	-1.59259
Sqle	-1.57135
Srm	-1.57097
scl0001259.1_60	-1.55067
Cpxm1	-1.53658
Rnaset2	-1.52336
Taf7l	-1.5066
D3Ucla1	-1.50564

Table S3: GO grouping of differentially regulated genes identified in murine placental JZ microarray analysis

#	Category	GO Reference	Expected	observed	False Discovery Rate (p-value)	Sub-Category
1	**Gene Ontology**	GO:0005576	8.39952	42	5.62151e-17	extracellular region
2	**Gene Ontology**	GO:0008152	36.408	76	5.44931e-11	metabolic process
3	**Gene Ontology**	GO:0048731	11.5921	39	1.38595e-10	system development
4	**Gene Ontology**	GO:0009987	57.2054	98	1.54034e-10	cellular process
5	**Gene Ontology**	GO:0005488	51.9179	91	4.0732e-10	binding
6	**Gene Ontology**	GO:0048856	12.9115	40	4.0732e-10	anatomical structure development
7	**Gene Ontology**	GO:0065008	7.4226	30	4.0732e-10	regulation of biological quality
8	**Gene Ontology**	GO:0050896	13.3899	40	9.8153e-10	response to stimulus
9	**Gene Ontology**	GO:0005515	27.097	59	3.65362e-09	protein binding
10	**Gene Ontology**	GO:0007275	14.1754	40	4.22509e-09	multicellular organismal development
11	**Gene Ontology**	GO:0044238	31.5083	64	6.63305e-09	primary metabolic process
12	**Gene Ontology**	GO:0048513	9.15991	30	2.55178e-08	organ development
13	**Gene Ontology**	GO:0032502	15.389	40	3.41949e-08	developmental process
14	**Gene Ontology**	GO:0065007	35.7181	66	1.2802e-07	biological regulation
15	**Gene Ontology**	GO:0019538	11.9749	33	2.06102e-07	protein metabolic process
16	**Gene Ontology**	GO:0003824	24.6295	51	2.65436e-07	catalytic activity
17	**Gene Ontology**	GO:0043170	25.3748	52	2.65436e-07	macromolecule metabolic process
18	**Gene Ontology**	GO:0005737	34.3031	63	3.27729e-07	cytoplasm
19	**Gene Ontology**	GO:0005623	72.7908	102	2.38784e-06	cell
20	**Gene Ontology**	GO:0044464	72.7858	102	2.38784e-06	cell part
21	**Gene Ontology**	GO:0044237	30.7328	56	2.89122e-06	cellular metabolic process
22	**Gene Ontology**	GO:0044424	49.108	76	7.79736e-06	intracellular part
23	**Gene Ontology**	GO:0005622	50.2914	77	8.59119e-06	intracellular
24	**Gene Ontology**	GO:0050789	33.5679	58	8.59119e-06	regulation of biological process

25	**Gene Ontology**	GO:0050794	31.9615	56	8.59119e-06	regulation of cellular process
26	**Gene Ontology**	GO:0032501	24.1763	46	1.03389e-05	multicellular organismal process
27	**Gene Ontology**	GO:0031323	13.8381	31	2.33533e-05	regulation of cellular metabolic process
28	**Gene Ontology**	GO:0044444	21.2657	41	2.72158e-05	cytoplasmic part
29	**Gene Ontology**	GO:0019222	14.7697	32	3.00647e-05	regulation of metabolic process
30	**Gene Ontology**	GO:0043226	41.9472	62	0.000397499	organelle
31	**Gene Ontology**	GO:0043231	36.9065	56	0.000469096	intracellular membrane-bounded organelle
32	**Gene Ontology**	GO:0043227	36.967	56	0.00047478	membrane-bounded organelle
33	**Gene Ontology**	GO:0043229	41.8264	60	0.0011161	intracellular organelle
34	**Gene Ontology**	GO:0044260	22.3685	36	0.00267099	cellular macromolecule metabolic process
35	**Gene Ontology**	GO:0023052	20.6463	31	0.0148365	signaling
36	**Gene Ontology**	GO:0005575	147.822	143	0.0169492	cellular_component
37	**Gene Ontology**	GO:0016020	37.3245	49	0.0214605	membrane
38	**KEGG**	-	1.57107	8	0.000247678	MAPK signaling pathway

Table S4: Deregulated genes with p value in qRT-PCR related to Fig. 4C

Gene	Deregulated in Tpbpa:Tfap2c$^{-/-}$ placentae	Mean fold change	p-value
Prl8a8	Down	181.18	<0.0001
Prl3a1	Down	20.74	0.022
Tpbpa	Down	20.49	0.0025
Pcdh12	Down	4.69	0.0019
Gjb3	Down	4.23	0.00016
Pl1	Unchanged	1.06	ns
Pl2	Down	3.36	0.004
Prl2c2	Down	3.04	0.011
Rgs5	Down	4.58	0.003
Pcsk6	Down	2.76	0.024
Tle3	Unchanged	1.3	ns
CtsQ	Unchanged	1.25	ns
P21	Up	3.34	0.00018
H19	Up	2.11	0.03
Tex 19.1	Down	2.22	0.03
Ascl2	Down	8.19	0.00054
Slc38a4	Down	2.61	<0.0001

Table S5: List of genotyping primers

Primers	Sequence 5'-3'
Cre F	TAAAGATATCTCACGTACTGACGGTG
Cre R	TCTCTGACCAGAGTCATCCTTAGC
Tfap2c P1	AACAGGTTATCATTTGGTTGGGATT
Tfap2c P2	CAATTTTGTCCAACTTCTCCCTCAA
Tfap2c P3	AATAGTCAGCCACCGCTTTACTAGG

Table S6: Primer Sequences for quantitative RT-PCR, ChIP and bisulfate sequencing.

Target name	Sequence 5'-3'	Reference
Tfap2c	F: CCTGCTCAGCTCCACGTC R: CCTCCATTTTTGGACTTTGC	
Tpbpa	F: CCAGCACAGCTTTGGACATCA R: AGCATCCAACTGCGCTTCA	
Hand1	F: CCCCTCTTCCGTCCTCTTAC R: CTGCGAGTGGTCACACTGAT	
Ascl2	F: GGTGACTCCTGGTGGACCTA R: TCCGGAAGATGGAAGATGTC	
Pl1	F: TGGAGCCTACATTGTGGTGG R: TGGCAGTTGGTTTGGAGGA	
Pl2	F: CCAACGTGTGATTGTGGTGT R: TGCCACCATGTGTTTCAGAG	
Prl2c2	F: TGCTCCTGGATACTGCTCCTA R: GGCTTGTTCCTTGTTTTCTGG	
Gcm1	F:CCATGTGAAACTGCCTCAGA R: CTTCCTCTGTGGAGCAGTCC	
Pcdh12	F: CTCCTGTCCAGCAAATCTCC R: TCTGCTTGACCACTAGGCTTG	
Gjb3	F: CTCCTCTGCTGTGGGTCTTG R: ATGCCGTGGAGTACTGGTTC	
P21	F: CCGTTGTCTCTTCGGTCCC R: CATGAGCGCATCGCAATC	(Choi et al., 2012)
Prl3a1	AGAGCGAAAGTGCATGTGTG GCACCTCTGTTTCCCTTCAG	(Reichmann et al., 2013)
Prl8a8	AAATTATGTGGGTGCCTGGA TCACGCAGAATTTGTCTGTTG	(Reichmann et al., 2013)
Rgs5	F: AGGCCCCTAAAGAGGTGAAC R: GACGGTTCCACCAGGTTCTT	(Mould et al., 2012)
Pcsk6	F: CCCAGGCAGAGACTCCAGAA R: GGCACACACTGGTCTGTAAAGT	(Mould et al., 2012)
Tle3	F: TGGTGAGCTTTGGAGCTGTT R: CGGTTTCCCTCCAGGAAT	(Villanueva et al., 2011)
CtsQ	F: GAGGCAGTAGTGGTCATCCC R: CAGTACTTCTTCCTCCGGACT	
H19	F: GAAATGGTGCTACCCAGCTCAT R:TTCAGCTTCACCTTGGAGCAG	(Sferruzzi-Perri et al., 2009)
Tex19.1	AAAATGGGCCACCCACATCTC CCACTGGCCCTTGGACCAGAC	(Reichmann et al., 2013)
Slc38a4	F: TGATTGGGATGTTAGTCTGAGG R: GGCCTGGGTTAAAATGTGTG	
Psg18	TGCAGGCAAACATTTCAGAG GAGTATGACAGGGGCCTCAA	(Reichmann et al., 2013)
Vefga	F: GCACATAGAGAGAATGAGCTTCC R: CTCCGCTCTGAACAAGGCT	(Jo et al., 2010)
Akt1	F: TCGTGTGGCAGGATGTGTAT R: ACCTGGTGTCAGTCTCAGAGG	
Dusp1	F: CATCCCTGTGGAGGACAACC R: CAGCATCCTTGATGGAGTCTATG	
Dusp4	F: TGCTTAAAGGTGGCTATGAGAGG	

	R: CTCATTGGTGCTGGGAGGTA	
Dusp6	F: CGAGAATAGCAGCGACTGGA R: TGAAGCCACCTTCCAGGTAGA	
B-Actin	F: TGTTACCAACTGGGACGACA R: GGGGTGTTGAAGGTCTCAAA	
Gapdh	F: ACCACAGTCCATGCCATCAC R: TCCACCACCCTGTTGCTGTA	
mouseChIP p21	F: TACGGGTGCCGTACATCAG R:AGCCTGGTCACCTTCCTACA	(Schemmer et al., 2013)
mouseChIP Dusp6	F: GCTGCAGCCTAGAAAGGATAG R: GCGGGAACTCAAGCGTAAA	
Human-TFAP2C	F: GGCCCAGCAACTGTGTAAAGA R: GCAGTTCTGTATGTTCGTCTCCAA	(Schemmer et al., 2013)
Human-DUSP1	F: GTACATCAAGTCCATCTGAC R: GGTTCTTCTAGGAGTAGACA	
Human-DUSP4	F: TGGCAATAAGGACTCGGAATA R:GGATCTGTGGGTTTCATCACT	
Bisulfite H19 CTCF3	F: GGGTTTTTTTGGTTATTGAATTTTAA R: AATACACACATCTTACCACCCCTATA	(Fauque et al., 2010)

Table S7: shRNA oligonucleotide sequence

Primer	Sequence
shRNA1 3'UTR	5´GATCCCCGGGAAGAGTTTGTTACCTATTCAAGAGATAGGTAACAAACTCT TCCCTTTTTA 3´GGGCCCTTCTCAAACAATGGATAAGTTCTCTATCCATTGTTTGAGAAGGG AAAAATTCGA
shRNA 2 ORF	5´GATCCCCCAGAAGAGCCAAATCGAAATTCAAGAGATTTCGATTTGGCTCT TCTGTTTTTA´ 3´GGGGTCTTCTCGGTTTAGCTTTAAGTTCTCTAAAGCTAAACCGAGAAGAC AAAAATTCGA

Supplementary References

Choi, I., Carey, T. S., Wilson, C. A. and Knott, J. G. (2012). Transcription factor AP-2gamma is a core regulator of tight junction biogenesis and cavity formation during mouse early embryogenesis. *Development*.

Fauque, P., Ripoche, M. A., Tost, J., Journot, L., Gabory, A., Busato, F., Le Digarcher, A., Mondon, F., Gut, I., Jouannet, P. et al. (2010). Modulation of imprinted gene network in placenta results in normal development of in vitro manipulated mouse embryos. *Hum Mol Genet* **19**, 1779-90.

Jensen, L. J., Kuhn, M., Stark, M., Chaffron, S., Creevey, C., Muller, J., Doerks, T., Julien, P., Roth, A., Simonovic, M. et al. (2009). STRING 8--a global view on proteins and their functional interactions in 630 organisms. *Nucleic Acids Res* **37**, D412-6.

Jo, J. O., Kim, S. R., Bae, M. K., Kang, Y. J., Ock, M. S., Kleinman, H. K. and Cha, H. J. (2010). Thymosin beta4 induces the expression of vascular endothelial growth factor (VEGF) in a hypoxia-inducible factor (HIF)-1alpha-dependent manner. *Biochim Biophys Acta* **1803**, 1244-51.

Kuckenberg, P., Buhl, S., Woynecki, T., van Furden, B., Tolkunova, E., Seiffe, F., Moser, M., Tomilin, A., Winterhager, E. and Schorle, H. (2010). The transcription factor TCFAP2C/AP-2gamma cooperates with CDX2 to maintain trophectoderm formation. *Mol Cell Biol* **30**, 3310-20.

Loots, G. G. and Ovcharenko, I. (2004). rVISTA 2.0: evolutionary analysis of transcription factor binding sites. *Nucleic Acids Res* **32**, W217-21.

Mould, A., Morgan, M. A., Li, L., Bikoff, E. K. and Robertson, E. J. (2012). Blimp1/Prdm1 governs terminal differentiation of endovascular trophoblast giant cells and defines multipotent progenitors in the developing placenta. *Genes Dev* **26**, 2063-74.

Reichmann, J., Reddington, J. P., Best, D., Read, D., Ollinger, R., Meehan, R. R. and Adams, I. R. (2013). The genome-defence gene Tex19.1 suppresses LINE-1 retrotransposons in the placenta and prevents intra-uterine growth retardation in mice. *Hum Mol Genet* **22**, 1791-806.

Schemmer, J., Arauzo-Bravo, M. J., Haas, N., Schafer, S., Weber, S. N., Becker, A., Eckert, D., Zimmer, A., Nettersheim, D. and Schorle, H. (2013). Transcription factor TFAP2C regulates major programs required for murine fetal germ cell maintenance and haploinsufficiency predisposes to teratomas in male mice. *PLoS One* **8**, e71113.

Sferruzzi-Perri, A. N., Macpherson, A. M., Roberts, C. T. and Robertson, S. A. (2009). Csf2 null mutation alters placental gene expression and trophoblast glycogen cell and giant cell abundance in mice. *Biol Reprod* **81**, 207-21.

Villanueva, C. J., Waki, H., Godio, C., Nielsen, R., Chou, W. L., Vargas, L., Wroblewski, K., Schmedt, C., Chao, L. C., Boyadjian, R. et al. (2011). TLE3 is a dual-function transcriptional coregulator of adipogenesis. *Cell Metab* **13**, 413-27.

Warde-Farley, D., Donaldson, S. L., Comes, O., Zuberi, K., Badrawi, R., Chao, P., Franz, M., Grouios, C., Kazi, F., Lopes, C. T. et al. (2010). The GeneMANIA prediction server: biological network integration for gene prioritization and predicting gene function. *Nucleic Acids Res* **38**, W214-20.